Primary productivity response to Heinrich events in the North Atlantic Ocean and Norwegian Sea

S. Nave, L. Labeyrie, J. Gherardi, N. Caillon, E. Cortijo, C. Kissel, F. Abrantes

Primary productivity response to Heinrich events in the North Atlantic Ocean and Norwegian Sea

S. Nave,[1,2] L. Labeyrie,[3,4] J. Gherardi,[3] N. Caillon,[3] E. Cortijo,[3] C. Kissel,[3] and F. Abrantes[1]

Received 21 June 2006; revised 7 March 2007; accepted 21 May 2007; published 14 September 2007.

[1] The last glacial was punctuated by several massive ice sheet surges into the North Atlantic that impacted surface water hydrology especially where icebergs melted. However, the links between variations in surface water hydrology and surface water productivity during these Heinrich events (HEs) remain uncertain. To address this issue, diatoms and organic carbon were examined across Heinrich event 1 (HE 1) and Heinrich event 4 (HE 4) in seven sediment cores spanning 40°N to 63°N latitude. Our results show low diatom abundances during HEs, consistent with decreased surface water productivity. Diatom dilution by increased sediment flux was tested by normalizing diatom abundance to a constant ^{230}Th flux. Although the particle rain rate was enhanced during HEs, this does not explain the sharp drop in diatoms. During HE 4, surface productivity decreased at all latitudes examined, probably because of strong, year-round stratification. The same inferred changes occurred during HE 1 within the area of maximum iceberg melting. However, at northern latitudes (above 50°N) the summer insolation increase of the glacial termination drove increased surface productivity during the whole period, including HE 1. Marine organic carbon, taken as independent proxy for export production, supports the diatom data. Trends shown by the productivity proxies evolve generally in parallel with the hydrographic proxies, with an increase in productivity when sea surface temperature increases.

Citation: Nave, S., L. Labeyrie, J. Gherardi, N. Caillon, E. Cortijo, C. Kissel, and F. Abrantes (2007), Primary productivity response to Heinrich events in the North Atlantic Ocean and Norwegian Sea, *Paleoceanography*, *22*, PA3216, doi:10.1029/2006PA001335.

1. Introduction

[2] The modern North Atlantic has large seasonal variations in ocean-atmosphere heat exchange, which drive strong fluctuations in the mixing depth, nutrient input and light availability within surface waters [*Marshall et al.*, 2001]. Each of these parameters influences primary productivity in the region [*Parsons and Lalli*, 1988; *Longhurst*, 1998].

[3] During the last glacial period, drastic changes in temperature, salinity and sea ice extent occurred in the North Atlantic on timescales of decades to centuries [*Bond et al.*, 1992]. This variability, originally recorded in Greenland ice cores [*Dansgaard et al.*, 1993] and now known as Dansgaard-Oeschger cycling (D-O events), is characterized by large-amplitude oscillations, each composed of a rapid (a few decades) shift to warm temperature (interstadials), and a slower cooling (several centuries) to severe cold periods (stadials). Six peculiar horizons span this period in North Atlantic sediment sequences [*Heinrich*, 1988]. These Heinrich events (HEs) are closely linked to some of the largest Dansgaard-Oeschger stadials recorded in ice cores. They are characterized by low concentrations of planktonic foraminifera and high abundances of ice-rafted detritus in the >150 μm size fraction [*Bond et al.*, 1992]. HE thickness decreases progressively from the Labrador Sea to the European margin within a band located between 40° and 55°N, the so-called "Ruddiman belt" [*Ruddiman*, 1977; *Grousset et al.*, 1993] (Figure 1). The HEs and their accumulation pattern probably represent accelerated melting of icebergs as they migrated southeast through the North Atlantic and met warmer subpolar water [*Death et al.*, 2006]. A critical outcome of these massive iceberg discharges was a large decrease in sea surface temperature (SST) and salinity [*Bond et al.*, 1992; *Cortijo et al.*, 1997], probably associated with a drastic drop or even a total shut down of deepwater convection in the northern Atlantic [*Oppo and Lehman*, 1995; *Vidal et al.*, 1997]. Several works have shown that, at the millennial scale, both HEs and stadial coolings (Dansgaard-Oeschger cycles) are associated with southern invasion of deep polar waters, disruption of the North Atlantic Current circulation, and a decrease in deep water ventilation [*Labeyrie et al.*, 1995; *Maslin et al.*, 1995; *Vidal et al.*, 1997; *Chapman and Shackleton*, 1998].

[4] The hydrographic changes during HEs may have affected the abundance and distribution of phytoplankton. *Ruddiman and McIntyre* [1981] suggested that in the presence of a large amount of melting icebergs as was the case in the glacial northern Atlantic, a steeper glacial

[1]Departamento de Geologia Marinha, Instituto Nacional de Engenharia, Tecnologia e Inovação, Alfragide, Portugal.
[2]Also at Laboratoire des Sciences du Climat et de l'Environnement, CEA/CNRS/UVSQ, Gif-sur-Yvette, France.
[3]Laboratoire des Sciences du Climat et de l'Environnement, CEA/CNRS/UVSQ, Gif-sur-Yvette, France.
[4]Also at Institut Universitaire de France, Université Versailles-St Quentin, Paris, France.

0883-8305/07/2006PA001335

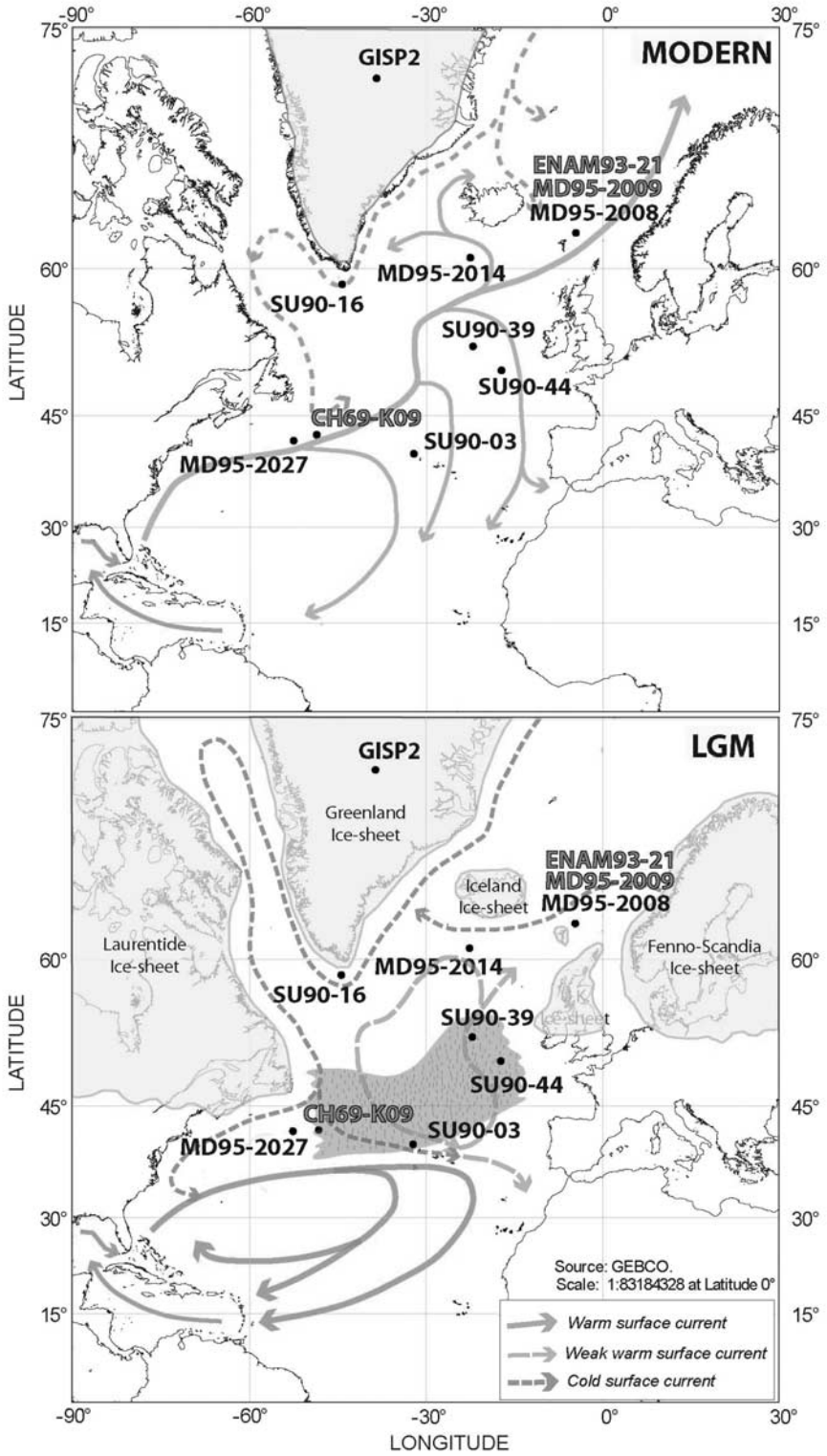
MODERN
LGM
GISP2
ENAM93-21
MD95-2009
MD95-2008
MD95-2014
SU90-16
SU90-39
SU90-44
CH69-K09
SU90-03
MD95-2027
Greenland Ice-sheet
Iceland Ice-sheet
Laurentide Ice-sheet
Fenno-Scandia Ice-sheet
Source: GEBCO.
Scale: 1:83184328 at Latitude 0°
Warm surface current
Weak warm surface current
Cold surface current
LATITUDE
LONGITUDE
-90°
-60°
-30°
0°
30°
75°
60°
45°
30°
15°

Figure 1

Table 1. Core Location, Water Depth, and Source Data

Core	Latitude, decimal deg	Longitude, decimal deg	Region	Water Depth, m	Source Data
SU90-16	58.22	−45.17	south of Greenland	2100	this study: diatoms, organic carbon, C/N; k [*Kissel et al.*, 1999]; percent detritics, δ^{18}O‰ *N. pachyderma* s. [*Elliot*, 1999]
MD95-2008	62.74	−3.99	north Faeroes	1016	this study: diatoms, organic carbon, C/N, IRD; k [*Kissel et al.*, 1999]
MD95-2009	62.74	−4.00	north Faeroes	1027	k [*Kissel et al.*, 1999]; δ^{18}O‰ *N. pachyderma* s., percent *N. pachyderma* s., percent *G. bulloides* [*Manthé*, 1998]
ENAM93-21	62.73	−3.89	north Faeroes	1020	this study: Mg/Ca; k, δ^{18}O‰ *N. pachyderma* s. [*Rasmussen et al.*, 1996]
MD95-2014	60.58	−22.08	south of Iceland	2397	this study: diatoms, organic carbon, C/N; k [*Kissel et al.*, 1999];detritics g^{-1}, δ^{18}O‰ *N. pachyderma* s., percent *N. pachyderma* s.; SST [*Manthé*, 1998]
GISP2	72.59	−38.46	Greenland Ice Sheet	-	*Blunier and Brook* [2001]
MD95-2027	41.74	−52.41	Newfoundland margin	4112	this study: diatoms, organic carbon, C/N, IRD; δ^{18}O‰ *N. pachyderma* s; k (C. Kissel, unpublished data, 2005)
CH69-K09	45.76	47.35	Newfoundland margin	4100	*Labeyrie et al.* [1999] and *Pastouret et al.* [1975]
SU90-03	40.05	−32.00	Azores	2475	this study: diatoms, organic carbon, C/N; lithics percent, *N. pachyderma* (percent), δ^{18}O ‰ *G. bulloides*, SST, δ^{13}C‰ *C. wuellerstorfi* [*Chapman and Shackleton*, 1998]
SU90-39	52.57	−21.93	northeast Thulean	3955	this study: diatoms, organic carbon, C/N, detritics (H1); k; percent detritics (H4); δ^{18}O‰ *N. pachyderma* s. [*Cortijo et al.*, 1997]; SST and alkenone abundance [*Villanueva et al.*, 1997]
SU90-44	50.02	−17.10	Porcupine Plain	4279	this study: diatoms, organic carbon, C/N; k [*Cortijo et al.*, 1997]; detritics g^{-1}; δ^{18}O‰ *N. pachyderma* s.; SST; percent *N. pachyderma* s. [*Labeyrie et al.*, 1995; *Vautravers et al.*, 1997]

pycnocline would have limited nutrient renewal at the surface and lowered productivity, thus reducting the amount of calcareous microfossils in sediment levels rich in ice-rafted detritus (IRD). This idea was later applied to the HEs [*Bond et al.*, 1992; *Broecker et al.*, 1992]. Conversely, increased diatom productivity has been linked to HEs [*Sancetta*, 1992]. In theory, such a rise in silica production might derive from an increase in the amount of drifting icebergs, which would be associated with larger input of dissolved silica and nutrients of continental origin or upwelled by iceberg plowing. Other factors may have affected productivity, as changes in summer insolation modulated by precession and obliquity, and surface temperature.

[5] We examine in the present work past changes in productivity and hydrography in 7 cores distributed through the northern Atlantic. The study is focused on Heinrich event 4 (HE 4) at about 39 cal ka B.P. and Heinrich event 1 (HE 1) at about 16 cal ka B.P. A significant decrease in SST and salinity occurred in the Ruddiman belt during the period of HE 4 [*Cortijo*, 1995] (Figure 1 and Table 1), while summer insolation and global ice volume were relatively constant. HE 1 at the opposite occurs at the beginning of the deglaciation, during a period of rapid increase in summer

Figure 1. Location of the cores presented in this study shown in black. The cores noted in grey stand for cores used as support data. The North Atlantic inferred surface circulation for the Last Glacial Maximum [*CLIMAP Project Members*, 1976; *Chapman and Maslin*, 1999] in comparison to the modern surface circulation [*McCartney et al.*, 1991; *Dickson and Brown*, 1994] is depicted. Approximate extension of ice sheets during the Last Glacial Maximum is depicted in grey [*CLIMAP Project Members*, 1976]. The dotted grey area defines the location of the ice-rafted detritus belt during isotope stage 2, where the rate of deposition of ice-rafted sand is greater than 300 mg cm^{-2} ka^{-1} [*Grousset et al.*, 1993], the so-called Ruddiman band [after *Ruddiman*, 1977]. Map created with PanMap Software (1998) (available at http://www.pangaea.de/Software/PanMap/).

Table 2. Chronostratigraphy for the Cores Located North of the Ruddiman Belt

Core	HE 1	HE 1 References	HE 4	HE 4 References	Calibration to Calendar Ages
SU90-16	^{14}C AMS dating of *N. pachyderma* s. (16.3 kyr and 17.6 kyr)[c]	*Elliot* [1999]	Laschamp event and *k* versus δ^{18}O GISP2 correlation	*Kissel et al.* [1999]	this study; H1 calibration: CALIB REV4.4.2 [*Stuiver and Braziunas*, 1993; *Stuiver et al.*, 1998a, 1998b; *Bard* 1998]
MD 95-2008[a]	^{14}C AMS dating of *N. pachyderma* s. in core MD95-2009 (16.1 kyr and 17.9 kyr)[c]	*Manthé* [1998]	Laschamp event and *k* versus δ^{18}O GISP2 correlation	*Kissel et al.* [1999]	this study;H1 calibration: CALIB REV4.4.2 [*Stuiver and Braziunas*, 1993; *Stuiver et al.*, 1998a, 1998b; *Bard* 1998]
MD 95-2014[b]	^{14}C AMS dating of *G. bulloides* and *N. pachyderma* s. (16.9 kyr and 18.1 kyr)[c]	*Manthé* [1998]	Laschamp event and *k* versus δ^{18}O GISP2 correlation	this study	this study;H1 calibration: CALIB REV4.4.2 [*Stuiver and Braziunas*, 1993; *Stuiver et al.*, 1998a, 1998b; *Bard* 1998]

[a]By previous correlation with the twin core MD95-2009.
[b]Even though more than one species has been used in one core, each level has been dated on monospecific foraminifera samples.
[c]Ages bracketing the interval.

insolation and a maximum in obliquity [*Berger*, 1978]. SST increases rapidly at the end of HE 1.

[6] A special attention has been given to the establishment of a common chronostratigraphy between the different cores, using the amount of ice-rafted detritus (IRD), low-field magnetic susceptibility (κ) and available ^{14}C dates. Productivity has been assessed by diatom abundance and organic carbon (C_{org}) content and surface hydrology constrained by δ^{18}O from planktonic foraminifera and their relative abundance. Dilution of biogenic remains by high IRD deposition has been estimated by ^{230}Th normalization [*Francois et al.*, 2004]. Our work demonstrates that this dilution does not explain the drastic drop in productivity observed during both events.

2. Study Area and Sediment Cores

[7] Locations of the 7 cores are reported in Figure 1. The SU cores were recovered in 1990 during the PALEOCINAT I cruise on board the R/V *Le Suroît* [*Labeyrie*, 1990], while the MD cores were collected in 1995 during IMAGES (International Marine Past Global Changes Study) cruise MD101 on board the R/V *Marion Dufresne* [*Bassinot and Labeyrie*, 1996]. These cores have been part of earlier studies for HE distribution [e.g., *Cortijo et al.*, 1997; *Chapman and Shackleton*, 1998; *Elliot*, 1999; *Kissel et al.*, 1999]. Three cores (MD95-2008, MD95-2014 and SU90-16) come from north of the main iceberg melting area. Core MD95-2008 (62.74°N; 3.99°W; 1016 m water depth, mwd) was collected in the southern Norwegian Sea, at the west side of the Faeroe-Shetland Channel. A detailed study of 2 other cores taken at the same location (ENAM93-21 [*Rasmussen et al.*, 1996] and MD95-2009 [*Manthé*, 1998]) demonstrated that surface productivity occurred throughout the last glacial, including the Heinrich events, which indicates that sea ice melted in summer at least in that area. Norwegian Sea was however characterized by reduced convection and slower deepwater circulation [*Rasmussen et al.*, 1996]. Core MD95-2014 (60.58°N; 22.08°W; 2397 mwd) has been retrieved west of Reykjanes Ridge, south of Iceland. It duplicates core SU90-33 [*Kissel et al.*, 1999]. Both cores have been extensively studied for their glacial records of surface hydrology, IRD distribution, and magnetic properties [*Cortijo et al.*, 1997; *Kissel et al.*, 1997, 1999]. Core SU90-16 (58.22°N; 45.17°W; 2100 m water depth) retrieved on the Eyrik drift, south of Greenland has been the object of similar studies [*Kissel et al.*, 1999; *Cortijo et al.*, 2005]. The IRD records of all these cores show a succession of peaks, part of them associated to the cold D/O stadials and Heinrich events, part to the history of local ice sheets.

[8] Four other cores were collected in the area directly under the trajectory of melting icebergs during HEs, between about 40°N and 55°N [*Grousset et al.*, 1993]. Their IRD records present the usual large amplitude peaks which define HEs. Cores SU90-39 (52.57°N; 21.93°W; 3955 mwd) and SU90-44 (50.02°N; 17.1°W; 4279 mwd) were collected in the eastern North Atlantic basin (Figure 1). Core MD95-2027 (41.74°N; 52.41°W; 4112 mwd) is located in the western Atlantic basin at the foot of the Newfoundland margin, and duplicates core CH69-K09, extensively studied over the period of the whole last glacial interglacial cycle [*Labeyrie et al.*, 1999]. Core SU90-03 (40°N; 32°W; 2475 mwd) is located on the western side of the Mid-Atlantic Ridge in the Azores region. It is near the southern limit of significant IRD deposition during the last glacial (Figure 1), where the IRD peaks corresponding to the HEs are well defined but of small magnitude.

3. Chronostratigraphy of the Heinrich Events

[9] The first issue to resolve is the construction of a precise chronostratigraphy (better that about 100 to 500 years, depending on sedimentation rate) for the different cores, particularly around the HEs, to put all the paleoproductivity reconstructions within the same time frame. Where possible, we have used available ^{14}C AMS dates of planktonic foraminifera tests (Tables 2 and 3) [*Manthé*, 1998; *Elliot*, 1999; *Labeyrie et al.*, 1999].

[10] Dating is fairly straightforward around HE 1 (~16 cal ka B.P.): The foraminifera δ^{18}O characteristic deglacial

Table 3. Age Model Sources for the Cores Located Within the Ruddiman Belt

Core	HE 1 and HE 4	References	Calibration to Calendar Ages
SU90-03	correlation using lithological and benthic (*Cibicidoides wuellerstorfi* and *Uvigerina* spp.) δ^{18}O data.	*Chapman and Shackleton* [1998]	*Chapman and Shackleton* [1998]
SU90-39	correlation of benthic foraminifera δ^{18}O (*Cibicidoides wuellerstorfi* and *Uvigerina peregrina*) records using Analyseries and NA87-22 as reference core. Radiocarbon ages were determined on *G. bulloides* and *N. pachyderma* s. in core NA87-22	*Labeyrie et al.* [1995]	this study
SU90-44	correlation of benthic foraminifera δ^{18}O (*Cibicidoides wuellerstorfi* and *Uvigerina peregrina*) records using Analyseries and NA87-22 as reference core. Radiocarbon ages were determined on *G. bulloides* and *N. pachyderma* s. in core NA87-22	*Labeyrie et al.* [1995]	this study
MD95-2027	correlation of *N. pachyderma* s. using Analyseries and CH69-K09 as reference core. Radiocarbon ages were determined on several species in core CH69-K09[a]	*Labeyrie et al.* [1999]	*Labeyrie et al.* [1999]

[a]The several species are *G. bulloides*, *N. pachyderma* s., *N. pachyderma* d., *G. inflata*, *Osangularia* and *Uvigerine*. Even though more than one species has been used in one core, each level has been dated on monospecific foraminifera samples.

record, and the IRD peaks are sufficiently constrained by available ^{14}C dates. Construction of a common chronostratigraphic timescale is more difficult around HE 4 (35 to 40 cal ka B.P.) because of low residual ^{14}C activity. The latter period is also characterized by strong variability in Earth's dipolar magnetic field, which affects the production of ^{14}C [*Laj et al.*, 2000]. Another problem is our incomplete knowledge of changes in reservoir age at high northern latitudes, which has often exceeded the standard 400 years used in many corrections [e.g., *Bard et al.*, 1990; *Waelbroeck et al.*, 2001]. For this reason, timescales for each core have been built independently, and HE time slices have been correlated on the basis of changes in sediment composition without specific reservoir age adjustments.

[11] As observed above, a direct correlation of the IRD signals between the different cores located north of the Ruddiman belt (SU90-16, MD95-2008 and MD95-2014) is not easy. Local iceberg discharges are not all synchronous between Greenland [*Elliot*, 1999] and the Fenno-Scandian ice sheet [*Rasmussen et al.*, 1996; *Dokken and Jansen*, 1999; *Elliot et al.*, 2001]. The chronostratigraphy for HE 4 was established following the NAPIS 75 stacked record of [*Laj et al.*, 2000] by correlation of the magnetic paleointensity record of the Laschamp event in these cores (located within D/O 10, between HE 4 and HE 5). Moreover, between 30 and 60 ka B.P. the changes on low-field magnetic susceptibility may be easily correlated between all high-latitude sediment cores [*Kissel et al.*, 1999]. The strong analogy between this common signal and the δ^{18}O curve of GISP2 ice core, at least around HE 4, facilitates regional correlations (auxiliary material Figure S1) [*Dokken and Jansen*, 1999; *Kissel et al.*, 1999].[1] Detailed correlation between magnetic susceptibility curves for each core and the δ^{18}O (‰) record of GISP2 ice core is shown in auxiliary material Figure S2. All correlations were done using the ANALYSERIES software [*Paillard et al.*, 1996].

[12] For cores from within the Ruddiman belt (SU90-39, SU90-44, MD95-2027), the HEs are well characterized by peaks of IRD, lows in foraminiferal concentration, and highs in bulk sediment density [*Heinrich*, 1988; *Bond et al.*, 1992; *Chi and Mienert*, 1996]. The IRD peaks are associated with large "low-field" magnetic susceptibility peaks because of a high amount of large magnetic multidomain particles [*Grousset et al.*, 1993; *Weeks et al.*, 1995]. HEs may be also recognized in sediment records at this latitudinal band by the characteristic foraminifera δ^{18}O signature of the two planktonic species *G. bulloides* and *N. pachyderma* s. [*Labeyrie et al.*, 1999] (See 4.5 δ^{18}O in planktic foraminifera).

4. Proxies and Methods

4.1. Diatoms and Paleoproductivity

[13] We use diatom abundances to reconstruct past productivity in surface waters. Diatoms are a dominant constituent of phytoplankton in this region [*Koç Karpuz and Schrader*, 1990], and are relatively abundant in North Atlantic glacial sediments [*Sancetta*, 1992]. Moreover, their production and diversity at high latitudes is great and clearly correlated to ocean currents [*Koç Karpuz and Schrader*, 1990]. As such, diatoms have been used successfully as paleoproductivity indicators for late Quaternary sediment in the North Atlantic [e.g., *Abrantes*, 2000]. Spores of the genus *Chaetoceros* are considered independently in this study. They are the major component of diatom blooms in the North Atlantic and may be interpreted as a regional spring bloom indicator [*Parsons and Lalli*, 1988].

[14] Diatom quantification was conducted following the counting procedures of *Schrader and Schuette* [1968]. Diatoms were counted in 100 randomly selected fields of view for one slide prepared from each sample (see auxiliary material). Diatom counts were converted to valves g^{-1} of sediment according to the following expression:

$$\text{Number of valves } g^{-1} = [(V_n \times (A_t/A_s)) \times (V/v)]/W, \quad (1)$$

where V_n is the number of valves counted, A_t is the area of the evaporation tray, A_s is the area of the slide counted, V is the volume of solution in the beaker, v is the volume of

[1]Auxiliary material data sets are available at ftp://ftp.agu.org/apend/pa/2006pa001335. Other auxiliary material files are in the HTML.

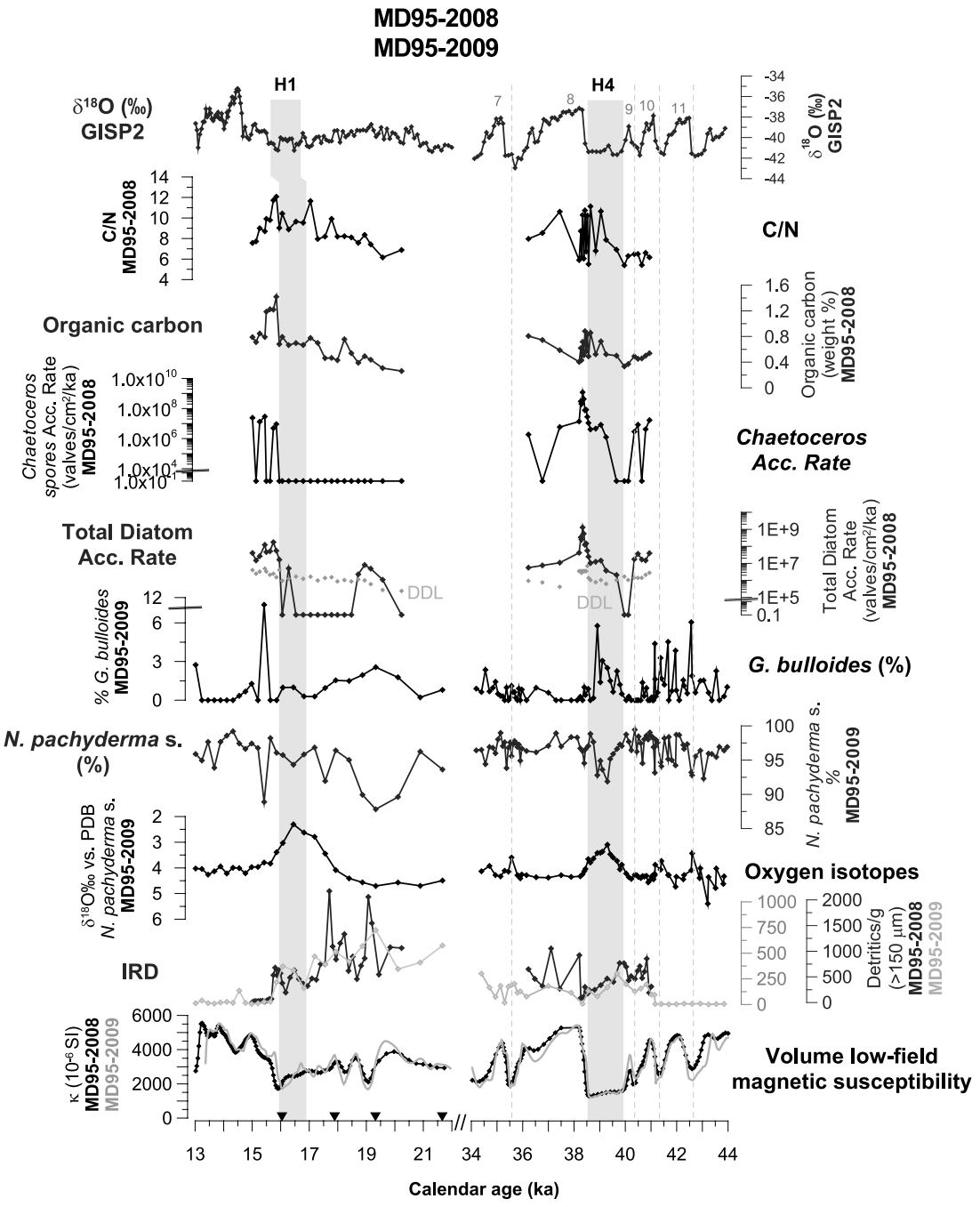

Figure 2. Cores MD95-2008 and MD95-2009: volume low-field magnetic susceptibility κ (10^{-6} SI) and detritus g^{-1} (>150 μm) for HE 1 and HE 4; δ^{18}O *N. pachyderma* s. versus Peedee belemnite (PDB), *N. pachyderma* s. (%) (taken as proxy for polar environment) for HE 1 and HE 4 for MD95-2009; *G. bulloides* (%) for HE 1 and HE 4 for MD95-2009 (taken as proxy for subpolar environment); diatom accumulation rate (DAR) (valves cm^{-2} ka^{-1}) (taken as proxy for productivity), *Chaetoceros* spores accumulation rate (valves cm^{-2} ka^{-1}) (taken as spring bloom indicator); and C/N ratio and organic carbon (wt %) for HE 1 and HE 4 time slices from core MD95-2008. HE 1 and HE 4 were identified on the basis of sedimentary characteristics. Triangles on the age axis stand for radiocarbon dates in core MD95-2009.

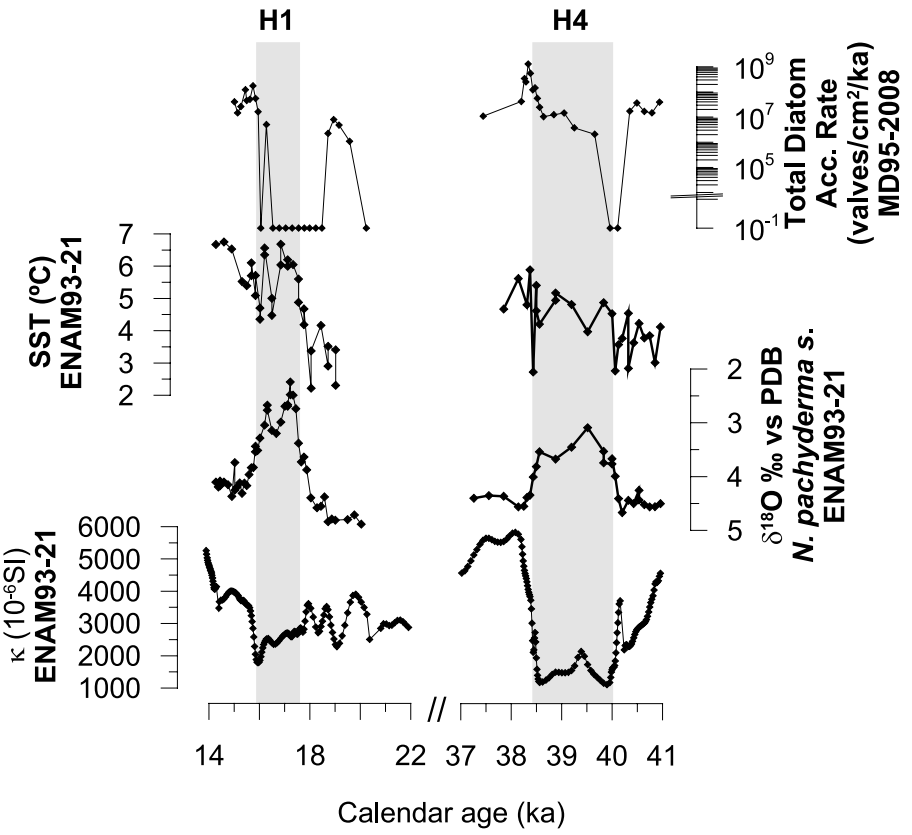

Figure 3. Core ENAM93-21 (same location as MD95-2008/2009): volume low-field magnetic susceptibility κ (10^{-6} SI); δ^{18}O *N. pachyderma* s. (‰) versus PDB; SST (°C) from *N. pachyderma* Mg/Ca ratios; and total diatom accumulation rate (valves cm^{-2} ka^{-1}) from core MD95-2008.

solution split into the evaporation tray, and W is the weight of raw sample. Diatom accumulation rate (DAR) and *Chaetoceros* spores accumulation rate, expressed as valves cm^{-2} ka^{-1}, were then obtained by the expression:

$$\text{valves cm}^{-2}\text{kyr}^{-1} = \text{valves g}^{-1} \times \text{bulk accumulation rate(BAR)} \cdot \left(\text{g cm}^{-2}\,\text{kyr}^{-1}\right) \quad (2)$$

where

$$\text{BAR}\left(\text{g cm}^{-2}\text{kyr}^{-1}\right) = \text{sedimentation rate}\left(\text{cm kyr}^{-1}\right) \times \text{dry bulk density(DBD)} \cdot \left(\text{g cm}^{-3}\right), \quad (3)$$

$$\text{DBD}\left(\text{g cm}^{-3}\right) = \text{wet bulk density} - [\text{porosity}/100 \times 1.026]. \quad (4)$$

Diatom accumulation rate (DAR) and *Chaetoceros* spores are expressed in logarithmic scale in Figures 2–8 and 10, to distinguish changes in the small DAR values during the cold stadials from the large DAR of the deglaciation and interstadials, which are several orders of magnitude higher.

[15] The "diatom detection limit" (DDL) for the diatom accumulation rate was determined for each sample and expressed as valves cm^{-2} ka^{-1}. Its value corresponds to the lowest achievable value using the counting procedures of *Schrader and Schuette* [1968] and the methodology of sample preparation used in this work.

4.2. Organic Carbon Content

[16] The organic carbon content in marine sediments has been used as a proxy for export production [*Rühlemann et al.*, 1999]. During HEs, however, an important fraction of organic carbon may be of terrigenous origin [*Villanueva et al.*, 1997]. To distinguish between marine and continental sources, we have measured the C/N ratios of organic carbon. Typical C/N values of marine organic carbon are between 7 and 9, while those of terrestrial organic carbon are commonly >15 [*Wefer et al.*, 1999].

[17] Total carbon and nitrogen were measured using a LECO CHNS-932 analyzer at INETI-DGM following the method described by *Manighetti* [1993] (see information in auxiliary material). The instrument was calibrated with sulfamethazine (carbon = 51.78%; nitrogen = 20.13%). Calibration standards and blanks were run before samples and between every 10 to 12 samples. The overall accuracy of the total carbon and nitrogen analyses is ± 3%.

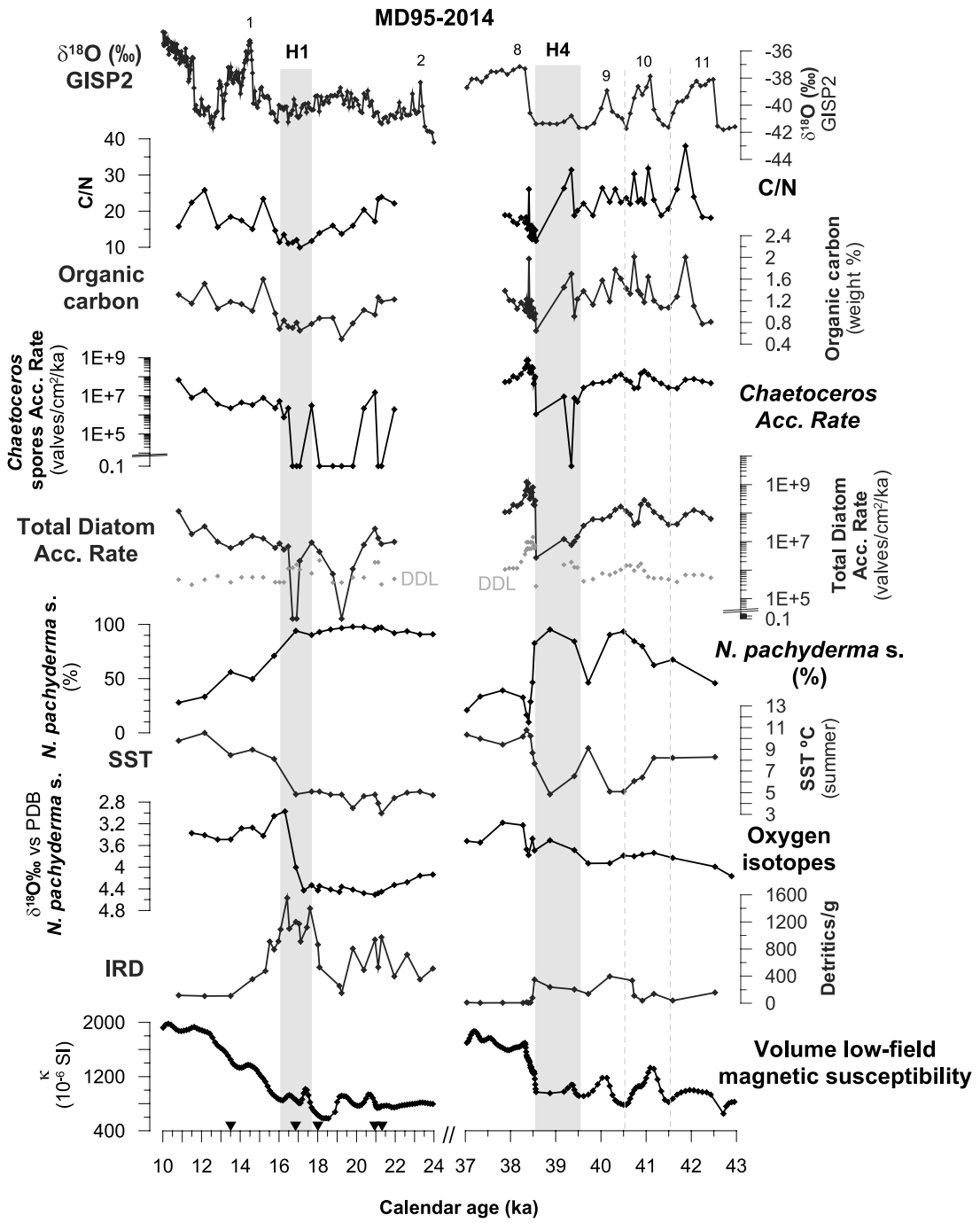

Figure 4. Core MD95-2014: volume low-field magnetic susceptibility κ (10^{-6} SI); IRD g^{-1}, $\delta^{18}O$ *N. pachyderma* s. versus PDB; SST °C (summer); *N. pachyderma* s. (%) (taken as proxy for polar environment); diatom accumulation rate (valves cm^{-2} ka^{-1}) (taken as proxy for productivity); *Chaetoceros* spores accumulation rate (valves cm^{-2} ka^{-1}) (taken as spring bloom indicator); organic carbon (wt %); and C/N ratio for HE 1 and HE 4 time slices. Triangles on the age axis stand for radiocarbon dates.

4.3. Ice-Rafted Detritus

[18] Lithic material greater than 150 μm in open ocean sediments typically represents ice-rafted debris (IRD) because it cannot be transported by ocean currents or winds [*Bond et al.*, 1992]. Sediment samples were sieved at 150 μm. The fraction >150 μm was distributed homogeneously in a counting tray. The relative abundance of lithic grains, foraminifera shells, volcanic grains and biogenic siliceous material was counted under a binocular microscope. In samples with low abundance of the coarse fraction

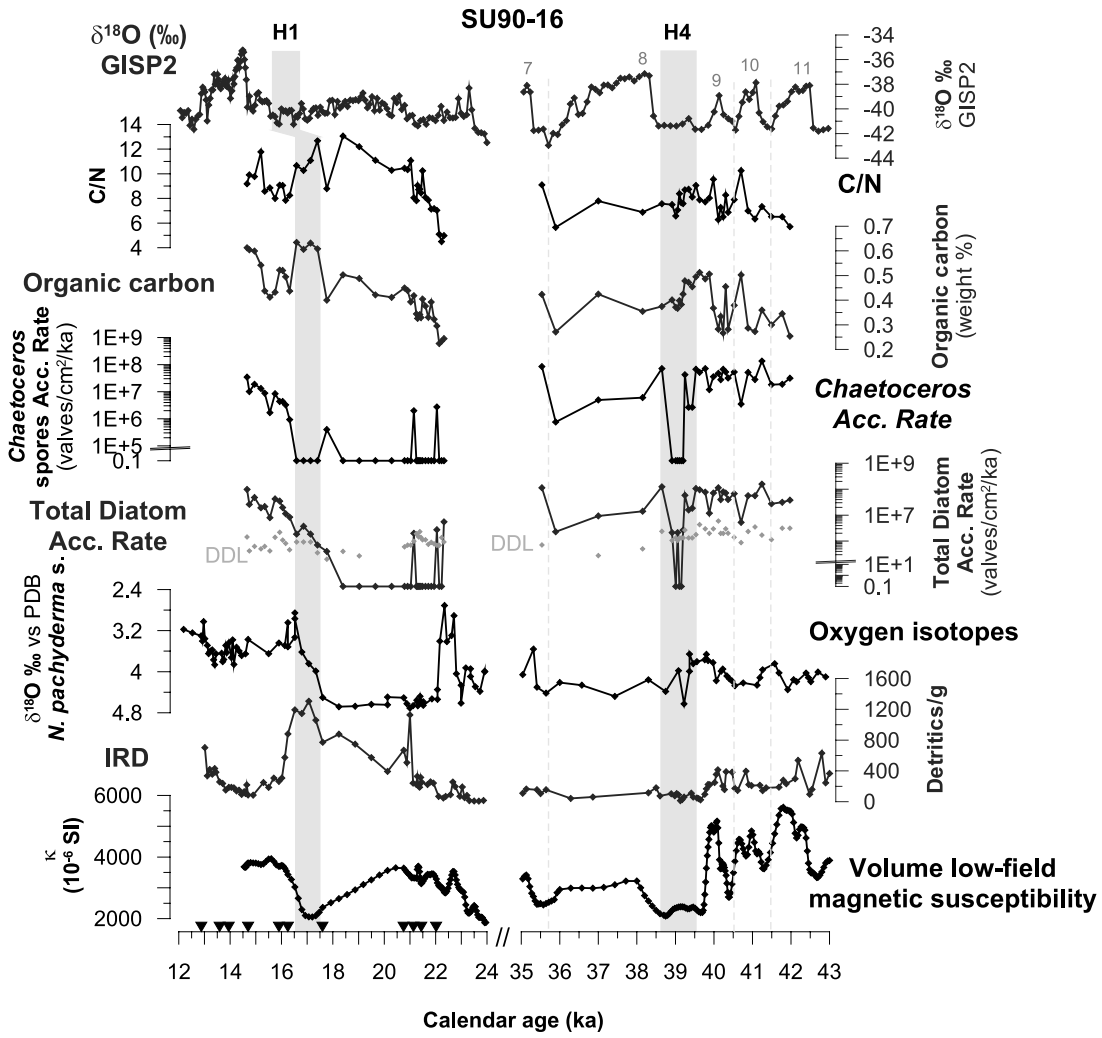

Figure 5. Core SU90-16: volume low-field magnetic susceptibility κ (10^{-6} SI); IRD g^{-1}; $\delta^{18}O$ *N. pachyderma* s. versus PDB; diatom accumulation rate (valves cm^{-2} ka^{-1}) (taken as proxy for productivity); *Chaetoceros* spores accumulation rate (valves cm^{-2} ka^{-1}) (taken as spring bloom indicator); organic carbon (wt %); C/N ratio for HE 1 and HE 4 time slices. Triangles on the age axis stand for radiocarbon dates.

(less than 300 grains), the whole sample was counted. Ice-rafted detritus abundance was then converted for each sample as numbers per gram and in percentage of the total counted particles.

4.4. The ^{230}Th Normalization

[19] Massive accumulation of ice-rafted debris will dilute the amount of biogenic material in sediment, and may explain some changes observed across HEs [*François and Bacon*, 1994]. Changes in particle flux and composition can be estimated by applying ^{230}Th normalization to the principal constituents of the sediment [*François and Bacon*, 1994]. We have used this method for core MD95-2027, which probably has the greatest dilution, as it is located near the source area for most of the ice-rafted material [*Grousset et al.*, 1993] (Figure 1). The method is based on the assumption that the flux of ^{230}Th scavenged to the seafloor is equivalent to the known rate of production in the overlying water column [*Bacon*, 1984]. Thus ^{230}Th activities in sediment can be translated into total preserved vertical mass fluxes or rain rates and corrected for sediment redistribution by bottom currents:

$$F = b^{*}z/^{230}\mathrm{Thxs},$$

where F is the normalized flux in g cm^{-2} ka^{-1}, b is the constant production rate of ^{230}Th in the water column (2.63×10^{-5} dpm cm^{-3} ka^{-1}), z in the water depth (cm), and ^{230}Thxs is the activity (dpm g^{-1}) in the sediment (see *Francois et al.* [2004] and *Henderson and Anderson* [2003] for recent reviews). Details on analytical procedures are given in the auxiliary material.

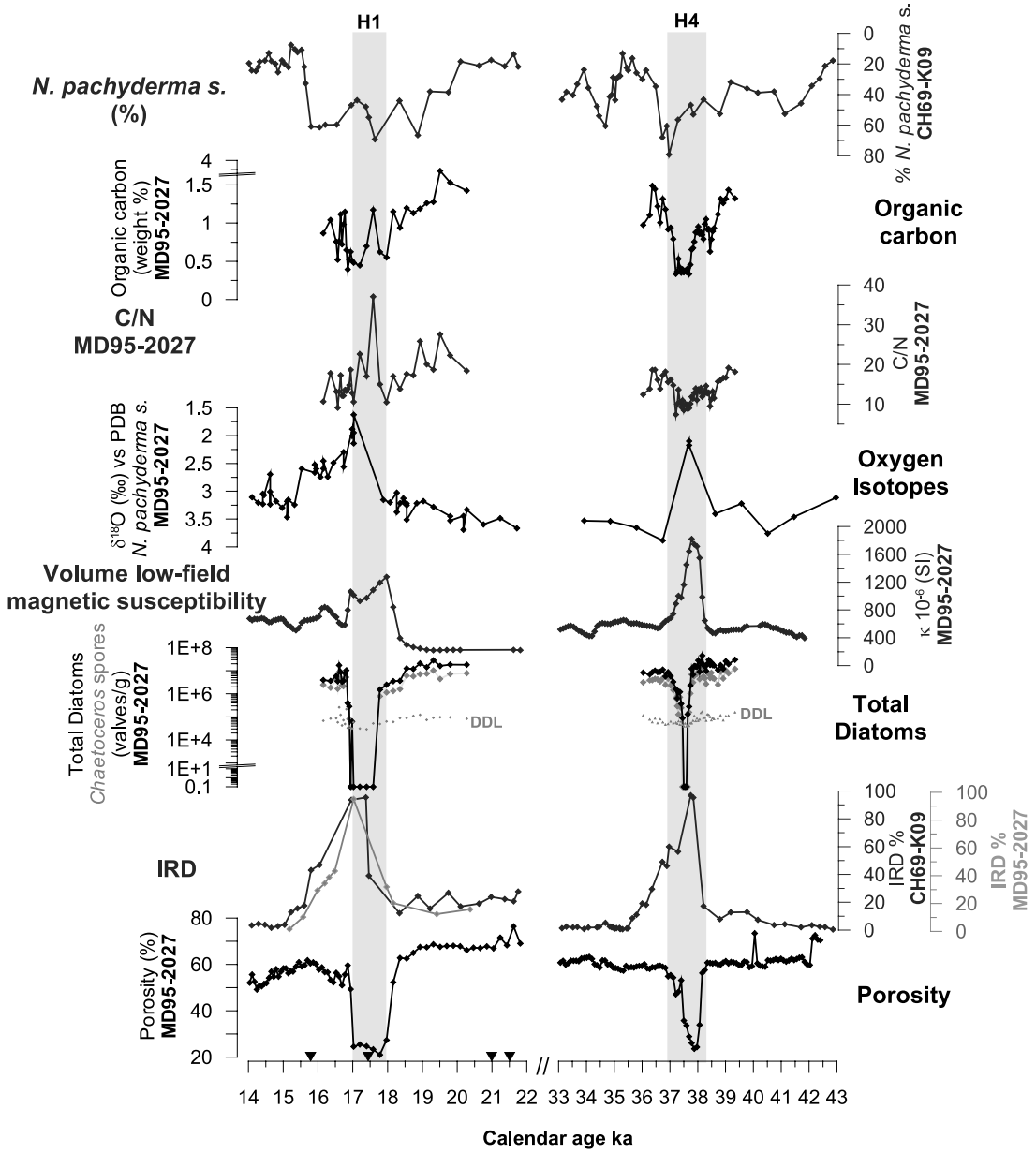

Figure 6. Cores MD95-2027 and CH69-K09: porosity (%); total diatom abundance (valves g^{-1}); volume low-field magnetic susceptibility κ (10^{-6} SI); C/N; organic carbon (wt %); total IRD (%); $\delta^{18}O$ *N. pachyderma* s. (‰) versus PDB; and *N. pachyderma* s. (%). Triangles on the age axis stand for radiocarbon dates in core CH69-K09.

4.5. Hydrographic Proxies: SST and $\delta^{18}O$ in Planktic Foraminifera

[20] Changes in SST were estimated from the relative abundance of the polar *Neogloboquadrina pachyderma* senestre (*N. pachyderma* s.). This species varies from over 90% for summer SST of 4°C or below, to less than 10% above 8°C [*Duplessy et al.*, 1991]). Reciprocally, the temperate species *Globigerina bulloides* varies from 0% north of the Polar Front, to about 30% or more south of the front [*Reynolds-Sautter and Thunell*, 1989]. For Norwegian Sea, SST was estimated by measuring the Mg/Ca ratio in *N. pachyderma* s., using the procedure of *de Villiers et al.* [2002] and *Barker et al.* [2003]. Samples of *N. pachyderma* s. were picked from the 200–250 μm fraction of core ENAM93-21 (at the same location of MD95-2008), and cleaned from clay and organic matter contamination by a succession of ultrasonic washing and oxidizing steps. Magnesium and calcium analyses were performed using a Varian Vista Pro Inductively Coupled Plasma Optical Emission Spectrometer (ICP-OES) housed at LSCE following the procedure developed by *de Villiers et al.* [2002]. Analytical precision of Mg/Ca was 0.5% for replicate runs of a

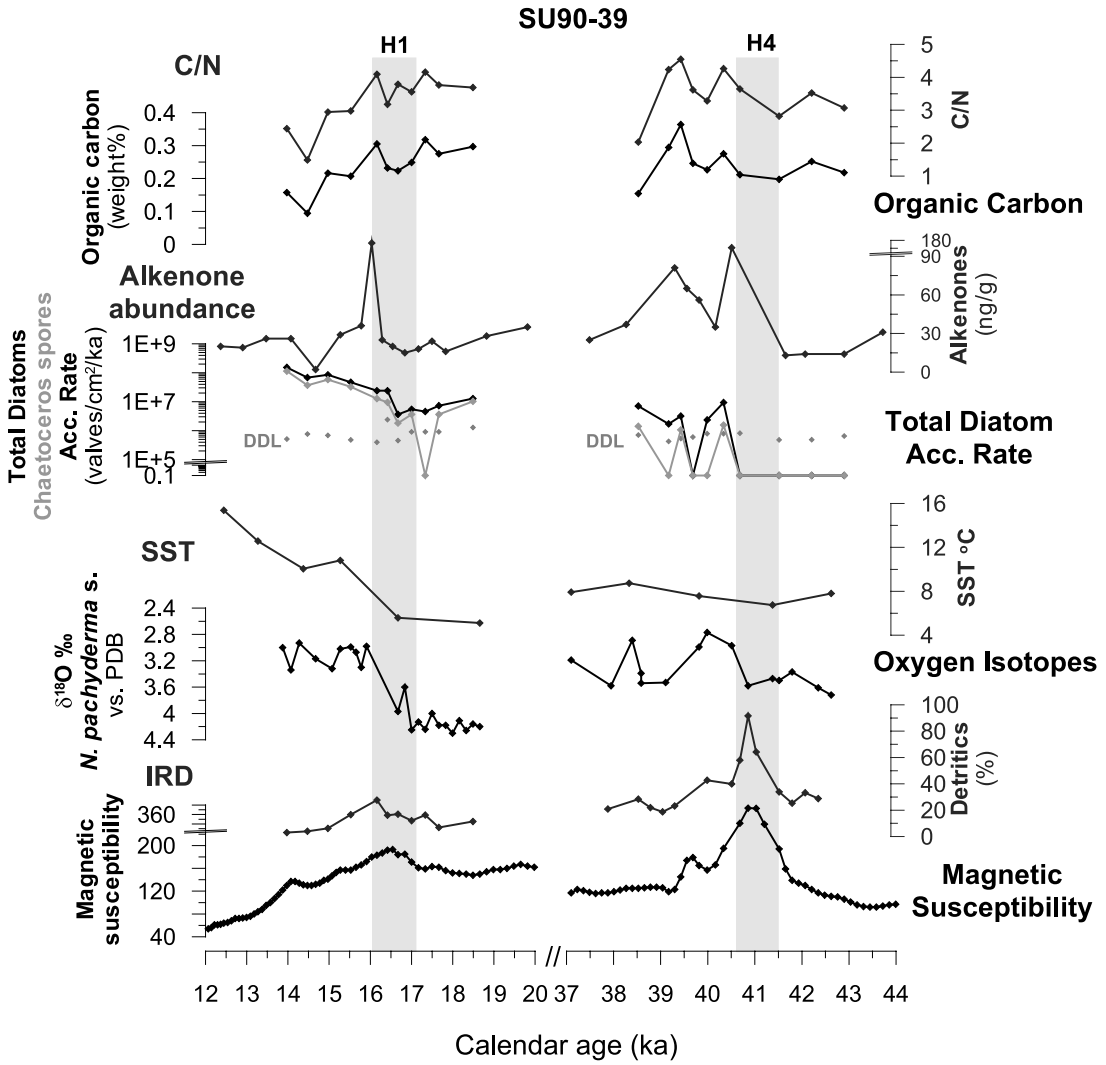

Figure 7. Core SU90-39: volume low-field magnetic susceptibility κ (10^{-6} SI); IRD (%); δ^{18}O *N. pachyderma* s. (‰) versus PDB; sea surface temperature (°C) estimates based on planktonic foraminifera species; diatom accumulation rate; *Chaetoceros* accumulation rate (valves cm^{-2} ka^{-1}); alkenone abundance; organic carbon (wt %); and C/N.

standard solution of Mg/Ca = 5.23 mmol mol^{-1} (1σ, RSD, n = 712), and external reproducibility 5.0% for *N. pachyderma* replicates (1σ, pooled RSD). To convert Mg/Ca values into SST, we used the calibration of *Elderfield and Ganssen* [2000], which was obtained using the same cleaning procedure. We have also analyzed in MD95-2008 the relative abundance of *G. bulloides*. Absent in polar waters, an increased abundance of this species should mark the arrival, even for a short summer period, of water from the vicinity of the polar front [*Bé*, 1960; *Reynolds-Sautter and Thunell*, 1989].

[21] Relative salinity changes and melt water events are recorded in the planktic foraminifera δ^{18}O. This parameter depends on surface water δ^{18}O and temperature (the foraminifera water $^{18}O/^{16}O$ fractionation changes by about $-0.25‰°C^{-1}$ [*Shackleton*, 1974]). *N. pachyderma* s. develops always in cold waters. During the HEs events, its δ^{18}O shows a large decrease, a record of the low-δ^{18}O seawater which tracks the effect of melting icebergs (of estimated δ^{18}O approximately −35‰ [*Labeyrie et al.*, 1995]). Such low δ^{18}O peak is observed in all the northern Atlantic and Norwegian Sea records when affected by melting icebergs. At the opposite, as we have seen, *G. bulloides* is a transitional species and may develop in a large range of temperatures, between 6° and 18°C [*Bé*, 1960; *Reynolds-Sautter and Thunell*, 1989]. During the HEs, its isotopic signal records, in addition to the sea water δ^{18}O decrease, the opposite effect of the drastic cooling associated with icebergs surges. The HEs signature corresponds here generally to a positive δ^{18}O shift. In the areas of the Polar Front and southward (the Ruddiman belt of maximum iceberg melting), when both species *G. bulloides* and *N. pachyderma* s. are simultaneously present in a sediment sample, their isotopic difference approaches zero

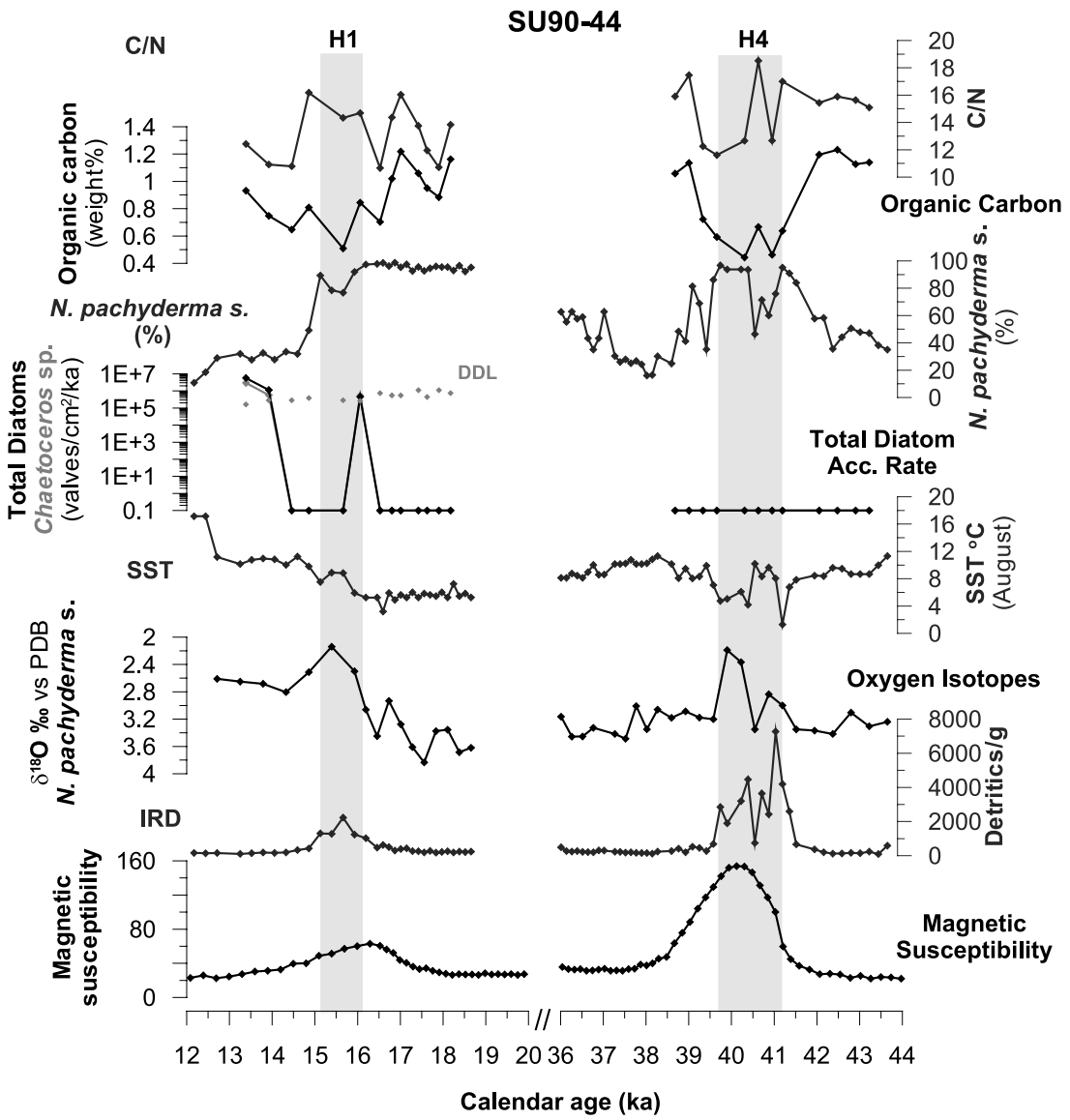

Figure 8. Core SU90-44: volume low-field magnetic susceptibility κ (10^{-6} SI); IRD g^{-1}; $\delta^{18}O$ *N. pachyderma* s. (‰) versus PDB; summer sea surface temperature (°C) estimates based on planktonic foraminifera species; diatom accumulation rate (valves cm^{-2} ka^{-1}), *N. pachyderma* s. (%); organic carbon (wt %); and C/N.

during HEs, which indicate a short common cold summer growth season. Out of HEs, their isotopic difference exceeds usually 1‰, in relation with local interannual and seasonal differences in growth environment. Thus these differences must have disappeared during HEs to explain the common $\delta^{18}O$ values [*Labeyrie et al.*, 1995; *Cortijo et al.*, 1997].

[22] Foraminifera $\delta^{18}O$ records have already been constructed for SU90-16, MD95-2009, MD95-2014, SU90-03, SU90-39, SU90-44 cores (Table 1). Oxygen isotope measurements for core MD95-2027 were done on specimens of *N. pachyderma* s. hand picked from the 250–315 μm fraction. Samples made up of 4 to 14 shells were analyzed following standard procedures using Finnigan "MAT251" and "Delta Plus" mass spectrometers housed at LSCE. Data are presented in standard delta notation relative to vPDB calibrated with respect to NBS19 [*Ostermann and Curry*, 2000]. The mean external reproducibility (1σ) of carbonate standards replicates is ±0.05‰ for $\delta^{18}O$ and $\delta^{13}C$.

5. Results

5.1. Northern Cores

[23] In Norwegian Sea (MD95-2008, Figure 2) there is a small but gradual increase, during HE 4, of diatom accumulation rate (DAR), *Chaetoceros* spores, C_{org} and *G. bulloides*, from a minimum at the start of the event to

a maximum at the beginning of interstadial 8, after the event. Even though a great variability is observed, C/N ratios are between 7 and 10, suggesting that the small increase in C_{org} is mainly of marine origin at this location. Background values for *N. pachyderma* s. relative abundance are always above 90% for the whole glacial period. However, an apparent decrease is observed within HE 4. The amount of IRD g^{-1} decreases also over that period, from a maximum just at the start of HE 4. This points to a progressive warming during HE 4, while staying in polar environment. In order to quantify the SST increase, we have measured *N. pachyderma* s. Mg/Ca ratio for the HE 4 period in core ENAM93-21 (Figure 3), located at the same position as MD95-2008 and MD95-2009 (and precisely tied to the MD95-2009 stratigraphy with *N. pachyderma s* $\delta^{18}O$ and magnetic susceptibility [*Elliot et al.*, 2001]. The Mg/Ca record is noisy, but does indicate a progressive $\sim$1°C warming during that period, which culminates after HE 4, at the beginning of Interstadial 8. Such warming is a small contribution to the *N. pachyderma* s. $\Delta\delta^{18}O$ shift of -1‰ (Figures 2 and 3), which mainly records the advection of surface water from the South with iceberg melt water contribution [*Cortijo et al.*, 1997].

[24] The records across HE 4 are different in core MD95-2014 south of Iceland (Figure 4). DAR and *Chaetoceros* spores decrease during the event, revealing a large drop in productivity. C_{org} content is highly variable, with a minimum at the end of HE 4, coincident with a C/N ratios >15, pointing to a terrigenous source. The SST temperature drops by about 4 degrees during HE 4 and the preceding stadial (with corresponding *N. pachyderma* s. (%), high values). The *N. pachyderma* s. apparent negative $\delta^{18}O$ anomaly is limited by the effect of SST cooling (-4°C changes the foraminiferal $\delta^{18}O$ by about +1‰).

[25] South of Greenland (core SU90-16, Figure 5), the changes in productivity are similar to what is seen south of Iceland (core MD95-2014, Figure 4), taking in account the about 1 kyr uncertainty in the precision of the stratigraphic correlations. The diatom signal decreases abruptly during HE 4. The spores of *Chaetoceros* also mark this dramatic drop on DAR. The C_{org} record presents some analogy with the DAR distribution but only during the HE 4. C/N ratios, with values between 6 and 10, suggest a marine origin for the C_{org}. SST estimates are not available for this core.

[26] For HE 1, the evolution of the productivity and hydrology present large similarities in the three northern cores (MD95-2008, MD95-2014 and SU90-16). In Norwegian Sea, *Chaetoceros* accumulation rate and DAR, as well as the changes in IRD, C_{org}, *N. pachyderma* s. and *G. bulloides* relative abundance, are smaller for HE 1 than for HE 4. The *N. pachyderma* s. Mg/Ca ratio indicates, as for HE 4 a mid-event warming of about 2°C, at the same time as a small increase in DAR (Figures 2 and 3). The *N. pachyderma* s. isotopic anomaly is of the same order, indicating again a large advection of isotopically light surface water from the South.

[27] In summary, for the northern cores, diatom productivity and the spores of the spring bloom indicator *Chaetoceros* evolve generally in parallel with the hydrographic proxies, with increase in productivity when SST increase. Organic carbon presents the same evolution, except when a high C/N indicates a large contribution from old continental carbon (as in core MD95-2014 at the beginning of HE 4). Productivity decrease significantly during the HEs in all records except for HE 1 in the south Greenland core, but this singularity may be due to the shortness of the productivity interruption. Morphology of the productivity signal depends however on the records. The minimum productivity appears early in the Norwegian Sea HE 4 record, followed by a progressive increase to the post Heinrich (interstadial 8). As we have seen, HE 1 occurs also within a trend to higher productivity parallel with warming surface waters and decreased IRD, in particular South of Iceland and off Greenland.

5.2. Ruddiman Belt Cores

[28] Cores MD95-2027, SU90-39, and SU90-44 (see Figure 1 for the location and Figures 6, 7, and 8, respectively, for the records) have clear minima in DAR during HE 4 and HE 1, in parallel with a large decrease in SST (in particular for MD95-2027, nearest the Laurentide ice sheet), synchronous with the increase in IRD and the *N. pachyderma* low $\delta^{18}O$ peak. As for the northern cores, the HE 1 drop occurs during a general trend of increased SST and productivity. The C_{org} signal of core MD95-2027 and SU90-39 resembles the diatom pattern, especially for the HE 4 time slice. Despite the good correlation between C_{org} and DAR distribution, C/N ratios are high (higher than 10) suggesting that at least part of the organic carbon has a terrigenous source. An undoubtedly terrigenous source for C_{org} is evident during HE 1, when a peak in C/N ratio reaches values close to 40 (Figure 6). In core SU90-39, the C_{org} signal does not present significant trend, and C/N ratio is within oceanic values. While analogous to MD95-2027 for HE 4 (within the uncertainty of our low-resolution sampling), that core presents some analogy with the northern cores for HE 1, with diatoms increasing within the IRD event, following the trend of the whole deglaciation.

[29] In core SU90-44, diatoms are absent and C_{org} stays low during both HEs, but the C/N ratio increases to values above 12, indicating a possible terrigenous source for the organic matter. Core SU90-03 (40°N 32°W) is located at the southern limit of the area of maximum IRD deposition [*Grousset et al.*, 1993]. In the modern ocean, this core is located within the North Atlantic central oligotrophic area, where surface productivity is low. Diatom analysis suggests that productivity was higher during glacial times (Figure 9). However during HEs, DAR decreases in parallel to the increase in the cold-water foraminifera species *N. pachyderma* s. (Figure 9). C_{org} is low (<0.4 wt %) and variable. Even though the IRD abundance is lower than 9%, a considerable drop in temperature and salinity changes was recorded at that latitude during HEs [*Cortijo et al.*, 1997; *Chapman and Shackleton*, 1998].

6. Discussion

6.1. Decreased Diatom Abundances and Their Cause

[30] In most of the cases, we observe a general decrease in mean diatom accumulation rate during HEs. We have attributed this decrease to a drop in primary productivity. However, two other factors may explain this decrease: (1) increased

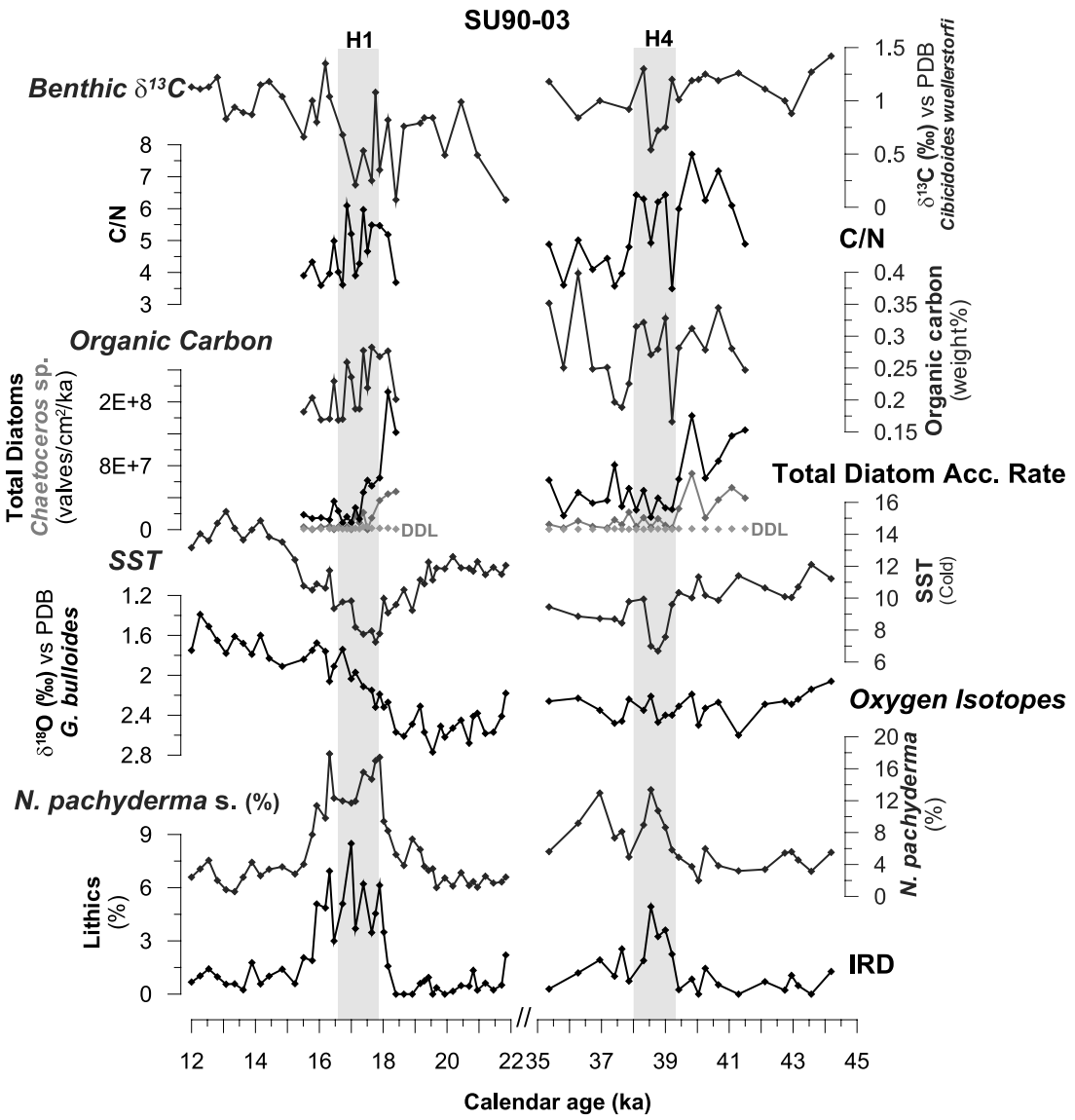

Figure 9. Core SU90-03: lithics (%); *N. pachyderma* s. (%); δ^{18}O *G. bulloides* (‰) versus PDB; winter sea surface temperature (°C) estimates based on planktonic foraminifera species; diatom accumulation rate (valves cm^{-2} ka^{-1}); organic carbon (wt %); C/N; and δ^{13}C *Cibicidoides wuellerstorfi* (‰) versus PDB.

dilution due to elevated fluxes of ice-rafted material within the events and (2) dissolution of diatom frustules.

[31] *François and Bacon* [1994] have used normalized ^{230}Th fluxes to show that massive increase in detrital fluxes occurred during HEs in the subpolar North Atlantic. We have used the same method to calculate changes in diatom fluxes through HE 1 in core MD95-2027, located within the zone of maximum IRD input [*Grousset et al.*, 1993] (Figure 10 and auxiliary material Table S1), thus where the dilution effect is maximum. Total sedimentary fluxes increased by about a factor of 10 in this core, which is consistent with *François and Bacon* [1994]. Correcting by the ^{230}Th method, normalized diatom fluxes still decreased by about a factor of 100 during the HE event. Such large changes in estimated normalized diatom flux could not be explained by changes in horizontal advection of sediment, or other causes for artifacts in the ^{230}Th normalization method [*Yu et al.*, 2001; *Francois et al.*, 2004]. Observations from core SU90-03 (located in the Azores region) also refutes a dilution hypothesis to explain lower DAR during HEs. As shown in Figure 9, IRD remains below 9% in that core. Nonetheless, there is a clear decrease in diatom accumulation rate and inferred productivity.

[32] Silica dissolution can be severe at the sediment water interface [*Broecker and Peng*, 1982]. However, an increase of bulk sediment accumulation rate during HEs would limit exchange with silica unsaturated bottom waters and better preserve fossil valves. Furthermore, a sharp decrease in bulk

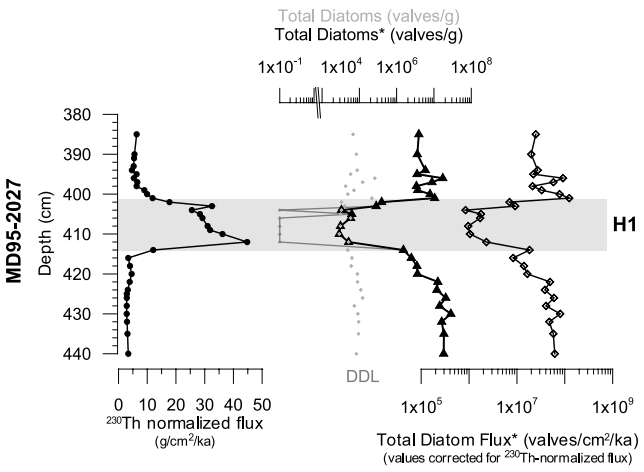

Figure 10. Core MD95-2027: ^{230}Th normalized flux (g cm^{-2} ka^{-1}), where ^{230}Th normalized flux is b* z/xsTh(0), with b = 2.63 $\times$ 10^{-5} (dpm cm^{-3} ka^{-1}), z is water column depth (cm), and xsTh(0) is the Th corrected from time decay [*François and Bacon*, 1994]; total diatom abundance (valves g^{-1}) and total diatom abundance* (valves g^{-1}), where values equal to zero were replaced by diatom detection limit (DDL) value; total diatom flux equal to total ^{230}Th normalized diatom flux (valves cm^{-2} ka^{-1}) and total diatom flux* equal to total diatoms * (valves g^{-1}) times ^{230}Th normalized flux at the same level.

sediment porosity marks the sediment rich in IRD (Figure 6). The associated lower water content would contribute to better opal preservation. Lastly, a higher contribution of silica-rich southern waters (Antarctic Bottom Water) has probably reached these latitudes during cold periods [*Marchitto et al.*, 2002], and this would have also favored silica preservation. Accordingly, we discount dissolution of diatom valves as an explanation for the sharp decrease in diatom abundance across HEs. We may also remark that, all other things being equal, diatom loss by dissolution should increase with lower biogenic silica flux to the bottom. This would not inverse the interpretation of the observed trend.

[33] An additional argument, which supports the interpretation of the changes in diatom accumulation rate in terms of productivity, is the general covariance with organic carbon content in the sediment, in the locations not affected by continental carbon input. However, the value of the C/N index as a quantitative discriminating factor has to be interpreted with caution in sediments containing low values of total organic carbon. In this case, a progressive masking of the original C/N ratio may occur leading to values in pelagic deposits between 5 and 15 [*Wagner and Dupont*, 1999]. Diagenesis may also be enhanced in well oxygenated and high porosity sediments.

[34] Our results show therefore that diatom productivity varied drastically during the last glacial, with a general drop in diatom accumulation rate and productivity during HEs. Although we studied only HE 4 and HE 1, *Pastouret et al.* [1975] for a site near MD95-2027 (core CH69-K09) published a similar decrease in diatom abundance during the periods of high IRD influx corresponding to each HE of the last glacial period (auxiliary material Figure S3). Our data is also in good agreement with *Thomas et al.* [1995]. These authors claimed for strongly reduced productivity during HEs in the Eastern Atlantic (50°–58°N), using the benthic foraminifera species (*Epistominella exigua* and *Alabaminella weddellensis*) that are known to grow opportunistically when a spring phytoplankton bloom results in seasonal deposition of phytodetritus on the seafloor.

[35] As we observed above, our general interpretation is however complicated by local differences and the varying analytical resolution between each core. All interstadials and post-Heinrich periods show large increase in productivity, which erase at least partially, in some of the records, the HEs productivity drop. The southern Norwegian Sea cores (ENAM93-20 and replicates) are typical example of local variability: they present a strong diatom minimum at the initiation of HE 4, but it is immediately followed by a productivity increase associated with the advection of the HE 4 meltwater and warmer northern Atlantic water. This increase corresponds to DAR values 2 orders of magnitude smaller that during the optimum of MIS 8. It does show, however, and in agreement with *Koç et al.* [1996] that diatom productivity increases with sea surface temperature. The response to HE 1 is also not as clear for the northern cores, perhaps because of the insufficient sampling resolution of some of the cores (SU90-16, SU90-39). The HE 1 event occurs within a well defined warming trend which follows the increase in summer insolation and continental ice volume decrease of the deglaciation. DAR again increase somewhat with the SST increase, but stays however at levels barely over detection limits, and more than 2 orders of magnitude below Holocene levels.

6.2. Changes in Diatom Production During HE 4

[36] The interval around HE 4 is well suited for studying the effects of iceberg discharges on surface water productivity independent of insolation forcing.

[37] In the modern North Atlantic, nutrients in the water column present a significant seasonal variability [*Longhurst*, 1998]. The seasonal succession of deep winter mixing followed by vernal stratification of the water column and development of productivity dominates the biological regime of the modern northern North Atlantic and Arctic seas [*Longhurst*, 1998]. A similar response occurred during interstadials of Marine Isotopic Stage (MIS) 3. The analogy between the records of DAR and *Chaetoceros* spores, suggests that productivity at these latitudes was rapidly renewed, and characterized mainly by seasonal spring blooms. In fact, diatom productivity during interstadials is about the same magnitude as found at present for surface sediments of the North Atlantic high latitudes [*Koç Kapuz and Schrader*, 1990]. The diatom productivity changes between stadials and interstadials observed in the northern cores are in good agreement with the results reported by [*Rasmussen et al.*, 1996] for the Norwegian Sea. The authors reported low foraminifera productivity during HEs and stadials and a

relatively warm fauna during Dansgaard-Oeschger interstadials, similar to the modern one in the Norwegian Sea.

[38] During HE 4, several factors may have contributed to decreased diatom productivity. Growth season was short and limited to a cold and low-salinity surface layer, as indicated by the converging $\delta^{18}O$ values for *N. pachyderma* s. and *G. bulloides* planktic foraminifera. We suggest that the low-salinity surface layer and associated stratification was renewed by melting icebergs, thus limiting the input of nutrients to the euphotic zone, and limiting productivity. A decrease in total light availability should be expected because of long winters with sea ice–covered water, short ice-free summers and increased loadings of atmospheric aerosols [*Denton et al.*, 2005].

6.3. Changes in Diatom Production During HE 1

[39] As discussed before, the HE 1 period has been chosen to test the effects of increased insolation and decreased ice sheet influence on productivity, just after the Last Glacial Maximum. At high latitudes, light availability in the ocean surface is very sensitive to seasonal effects, constituting one of the limitations for phytoplankton blooms [*Sverdrup*, 1953]. During MIS2, light was reduced by lower summer insolation and higher sea ice cover conditions. At the opposite HE 1 lies on the onset of deglaciation that coincides with a maximum in obliquity and a period of increasing summer insolation at high northern latitudes, peaking between 12 and 15 ka B.P. [*Berger*, 1978]. Productivity is minimum in all the northern cores at the end of the Last Glacial Maximum, and tends to increase during deglaciation in parallel with the increase in insolation, the HE 1 drop being more or less marked depending on the cores. At the opposite, south of about 50°N, within the Ruddiman belt, HE 1 presents a well marked minimum in productivity, and its increase occurs only at the end of the event. It is tempting to attribute this latitudinal difference to the changes in the relative importance of insolation versus surface hydrology to control primary productivity, insolation change playing its major role only at high northern latitudes, where light is limited or absent for a large part of the year.

6.4. The $^{231}Pa/^{230}Th$ Ratio in Sediments as Proxy for Changes in Circulation

[40] An implication of our work concerns a different proxy, recently developed to quantify the changes in Atlantic Meridian Overturning Circulation (AMOC) during HEs: the excess $^{231}Pa/^{230}Th$ ratio in the sediments. *McManus et al.* [2004] and *Gherardi et al.* [2005] have shown that this ratio increases in the deep North Atlantic sediments to the production value in the water column (0.093) during HE 1, to be compared to about half (0.04 to 0.06) before and after that period. They interpret that change as due to a drop in the export of the more soluble ^{231}Pa to the Southern Ocean, deriving from a significant decrease of the AMOC. That interpretation could be challenged if the HE 1 period corresponded to an increase in diatom valves production, as it would trap and transport ^{231}Pa efficiently to the bottom sediment [*Chase et al.*, 2002]. Our results prove, at the opposite, an overall decrease in diatom productivity and flux of opal to the sediment, thus supporting the interpretation of *McManus et al.* [2004].

7. Conclusions

[41] Massive iceberg discharges during HEs impacted sea surface hydrology in the North Atlantic [*Cortijo et al.*, 1997]. They have caused a significant drop in sea surface temperature and salinity, but the implication of these changes over oceanic productivity remained unclear because of the lack of high-resolution data. Two contrary hypotheses have been developed in the past. The first school interpreted the observed low abundance of microfossils in the sediment during these periods as drastic decrease in productivity. The second considered that diatom productivity had probably increased (an effect of increased nutrient input from the continents), but it has not been recorded in the sediments [*Sancetta*, 1992]. In the present study, we have addressed these issues for two different HEs, HE 1 and HE 4, in conducting a detailed analysis in 7 sediment cores from the northern Atlantic and Norwegian Sea. We have been able to show the following:

[42] 1. In agreement with past studies [*François and Bacon*, 1994], ^{230}Th flux normalization show an increase by about 10 folds of the particle rain rates during HE 1 in the area of maximum continental detritus input, while ^{230}Th normalized diatom flux decrease by about 2 orders of magnitude. Thus dilution by detritus does not explain the decrease of diatom abundance during HEs.

[43] 2. During interstadials, diatom abundance is 10^6–10^7 valves g^{-1} of sediment, similar to that in surface sediments from the Greenland, Iceland and Norwegian Seas [*Koç Karpuz and Schrader*, 1990]. Diatom productivity appears driven by the same mechanism that occurs in the modern North Atlantic: vernal thermal stratification of surface waters, after strong winter mixing, allowing the development of rapid blooms.

[44] 3. During HE 4, our diatom data (diatom accumulation rate) suggest that siliceous phytoplankton productivity decreased drastically at all latitudes, in contradiction to the *Sancetta* [1992] model. This decrease could have resulted from at least two factors which may have added their effect: a reduced salinity at the surface with an associated strong, perhaps year-round, halocline, which reduced nutrient supply, and surface water cooling or a reduction in light availability by floating ice. A similar conclusion has been proposed for carbonate productivity [*Bond et al.*, 1992; *Broecker et al.*, 1992].

[45] 4. The evolution of productivity over the HE 1 period differs at high northern latitudes (higher than 50°N) and more south, in the Ruddiman belt where a major part of the iceberg melted. In the northern latitudes, productivity increases progressively with the increase in insolation, after about 16 ka B.P. HE 1 appears as a short interruption in this trend, or does not have visible effect. Light appears therefore a major forcing function for productivity at these latitudes. At the opposite, in the 40°–50°N latitudinal band,

a drastic decrease of productivity is observed during HE 1, in phase with the changes in surface hydrology, and similarly to what happens during HE 4.

[46] **Acknowledgments.** Special thanks are due to J.-C. Duplessy for constructive discussions on the first version of the manuscript. Acknowledgement is also due to Elisabeth Michel and Claire Waelbroeck for helpful discussion on age model establishment and to António Ferreira for valuable discussions and cooperation. We thank Brigitte Lecoat, Jérôme Tessier, and Fabien Dewilde for processing isotopic measurements; Quentin Gautier and Hélène Rebaubier for Mg/Ca analyses; and Cremilde Monteiro for processing organic carbon analyses. Gulay Isguder and Apolónia Inês are acknowledged for technical assistance. Thanks go to Mark Chapman for his helpful comments and revision. We are especially indebted to Gerald Dickens for the thoroughness of his editorial support and detailed suggestions to increase the quality and readability of the manuscript. LSCE is supported by CEA, CNRS, and PNEDC. S. Nave acknowledges funding from Fundação para a Ciência e a Tecnologia (grant SFRH/BD/11742/2003) and INGMAR project through the "Programa de Intervenção nos Laboratórios do Estado do Ministério da Ciência e Tecnologia." Additional funding has been provided by the French Programme National de la Dynamique du Climat, Centre National de la Recherche Scientifique, and Commissariat à L'Energie Atomique. Coring cruises are funded by IFREMER and IPEV. This is LSCE publication number 2613.

References

Abrantes, F. (2000), 200,000 yr diatom records from Atlantic upwelling sites reveal maximum productivity during LGM and a shift in phytoplankton community structure at 185,000 yr, *Earth Planet. Sci. Lett.*, *176*, 7–16.

Bacon, M. P. (1984), Glacial to interglacial changes in carbonate and clay sedimentation in the Atlantic Ocean estimated from ^{230}Th measurements, *Isot. Geosci.*, *2*, 97–111.

Bard, E. (1998), Geochemical and geophysical implications of the radiocarbon calibration, *Geochim. Cosmochim. Acta*, *62*, 2025–2038.

Bard, E., B. Hamelin, R. G. Fairbanks, and A. Zindler (1990), Calibration of the ^{14}C timescale over the past 30,000 years using mass spectrometric U-Th ages from Barbados corals, *Nature*, *345*, 405–410.

Barker, S., M. Greaves, and H. Elderfield (2003), A study of cleaning procedures used for foraminiferal Mg/Ca paleothermometry, *Geochem. Geophys. Geosyst.*, *4*(9), 8407, doi:10.1029/2003GC000559.

Bassinot, F., and L. Labeyrie (1996), Les rapports de campagne à la mer à bord du *Marion-Dufresne*: Campagne IMAGES MD 101, *Rep. 96-1*, 217 pp., Inst. Fr. pour la Rech. et la Technol. Pol., Plouzane, France.

Bé, A. W. H. (1960), Ecology of recent planktonic foraminifera. part II: Bathymetric and seasonal distributions in the Sargasso Sea off Bermuda, *Micropaleontology*, *6*, 373–392.

Berger, A. L. (1978), Long-term variations of daily insolation and quaternary climatic changes, *J. Atmos. Sci.*, *35*, 2362–2367.

Blunier, T., and E. J. Brook (2001), Timing of millennial-scale climate change in Antarctica and Greenland during the last glacial period, *Science*, *291*, 109–112.

Bond, G., et al. (1992), Evidence for massive discharges of icebergs into the North Atlantic ocean during the last glacial period, *Nature*, *360*, 245–249.

Broecker, W. S., and T. H. Peng (1982), *Tracers in the Sea*, Eldigio, Palisades, N. Y.

Broecker, W., G. Bond, M. Klas, E. Clark, and J. McManus (1992), Origin of the northern Atlantic's Heinrich events, *Clim. Dyn.*, *6*, 265–273.

Chapman, M. R., and M. A. Maslin (1999), Low-latitude forcing of meridional temperature and salinity gradients in the subpolar North Atlantic and the growth of glacial ice sheets, *Geology*, *27*, 875–878.

Chapman, M. R., and N. J. Shackleton (1998), Millennial-scale fluctuations in North Atlantic heat flux during the last 150,000 years, *Earth Planet. Sci. Lett.*, *159*, 57–70.

Chase, Z., R. F. Anderson, M. Q. Fleisher, and P. W. Kubik (2002), The influence of particle composition and particle flux on scavenging of Th, Pa and Be in the ocean, *Earth Planet. Sci. Lett.*, *204*, 215–229.

Chi, J., and J. Mienert (1996), Linking physical property records of Quaternary sediments to Heinrich events, *Mar. Geol.*, *131*, 57–73.

CLIMAP Project Members (1976), The surface of the ice-age Earth, *Science*, *191*, 1131–1137.

Cortijo, E. (1995), La Variabilité climatique rapide dans l'Atlantique nord depuis 128,000 ans: Relations entre les calottes de glace et l'océan de surface, Ph.D. thesis, Univ. de Paris-Sud, Orsay, France.

Cortijo, E., L. Labeyrie, L. Vidal, M. Vautravers, M. Chapman, J.-C. Duplessy, M. Elliot, M. Arnold, J.-L. Turon, and G. Auffret (1997), Changes in sea surface hydrology associated with Heinrich event 4 in the North Atlantic Ocean between 40° and 60°N, *Earth Planet. Sci. Lett.*, *146*, 29–45.

Cortijo, E., J.-C. Duplessy, L. Labeyrie, J. Duprat, and D. Paillard (2005), Heinrich events: Hydrological impact, *C. R. Geosci.*, *337*, 897–904.

Dansgaard, W., et al. (1993), Evidence for general instability of past climate from a 250-kyr ice-core record, *Nature*, *364*, 218–220.

Death, R., M. J. Siegert, G. R. Bigg, and M. R. Wadley (2006), Modelling iceberg trajectories, sedimentation rates and meltwater input to the ocean from the Eurasian ice sheet at the Last Glacial Maximum, *Palaeogeogr. Palaeoclimatol. Palaeoecol.*, *236*, 135–150.

Denton, G. H., R. B. Alley, G. C. Comer, and W. S. Broecker (2005), The role of seasonality in abrupt climate change, *Quat. Sci. Rev.*, *24*, 1159–1182.

de Villiers, S., M. Greaves, and H. Elderfield (2002), An intensity ratio calibration method for the accurate determination of Mg/Ca and Sr/Ca of marine carbonates by ICP-AES, *Geochem. Geophys. Geosyst.*, *3*(1), 1001, doi:10.1029/2001GC000169.

Dickson, R. R., and J. Brown (1994), The production of North Atlantic Deep Water: Sources, rates, and pathways, *J. Geophys. Res.*, *99*(C6), 12,319–12,341.

Dokken, T. M., and E. Jansen (1999), Rapid changes in the mechanism of ocean convection during the last glacial period, *Nature*, *401*, 458–461.

Duplessy, J.-C., L. Labeyrie, A. Juillet-Leclerc, F. Maitre, J. Duprat, and M. Sarnthein (1991), Surface salinity reconstruction of the North Atlantic Ocean during the last glacial maximum, *Oceanol. Acta*, *14*, 311–324.

Elderfield, H., and G. Ganssen (2000), Past temperature and δ^{18}O of surface ocean waters inferred from foraminiferal Mg/Ca ratios, *Nature*, *405*, 442–445.

Elliot, M. (1999), Variabilité millénaire du climat et de l'hydrologie de l'océan atlantique nord lors de la dernière période glaciaire (60,000–10,000 ans), report, Univ. de Paris-Sud, Orsay, France.

Elliot, M., L. Labeyrie, T. M. Dokken, and S. Manthé (2001), Coherent patterns of ice rafted debris deposits in the Nordic regions during the last glacial (10–60 ka), *Earth Planet. Sci. Lett.*, *194*, 151–163.

François, R., and M. P. Bacon (1994), Heinrich events in the North Atlantic: Radiochemical evidence, *Deep Sea Res., Part I*, *41*, 315–334.

Francois, R., M. Frank, M. M. Rutgers van der Loeff, and M. P. Bacon (2004), ^{230}Th normalization: An essential tool for interpreting sedimentary fluxes during the late Quaternary, *Paleoceanography*, *19*, PA1018, doi:10.1029/2003PA000939.

Gherardi, J.-M., L. Labeyrie, J. F. McManus, R. Francois, L. C. Skinner, and E. Cortijo (2005), Evidence from the northeastern Atlantic basin for variability of the meridional overturning circulation through the last deglaciation, *Earth Planet. Sci. Lett.*, *240*, 710–723.

Grousset, F. E., L. Labeyrie, J. A. Sinko, M. Cremer, G. Bond, J. Duprat, E. Cortijo, and S. Huon (1993), Patterns of ice-rafted detritus in the glacial North Atlantic, *Paleoceanography*, *8*, 175–192.

Heinrich, H. (1988), Origin and consequences of cyclic ice rafting in the northeast Atlantic Ocean during the past 130,000 years, *Quat. Res.*, *29*, 142–152.

Henderson, G. M., and R. F. Anderson (2003), The U-series toolbox for paleoceanography, *Rev. Mineral. Geochem.*, *52*, 493–531.

Kissel, C., C. Laj, B. Lehman, and L. Labeyrie (1997), Changes in the strength of the Iceland-Scotland Overflow Water in the last 200,000 years: Evidence from magnetic anisotropy analysis of core SU90-33, *Earth Planet. Sci. Lett.*, *152*, 25–36.

Kissel, C., C. Laj, L. Labeyrie, T. Dokken, A. Voelker, and D. Blamart (1999), Rapid climatic variations during climatic stage 3: Magnetic analysis of sediments from Nordic Seas and North Atlantic, *Earth Planet. Sci. Lett.*, *171*, 489–502.

Koç Karpuz, N., and H. Schrader (1990), Surface sediment diatom distribution and Holocene paleotemperature variations in the Greenland, Iceland and Norwegian Sea, *Paleoceanography*, *5*, 557–580.

Koç, N., E. Jansen, M. Hald, and L. Labeyrie (1996), Late glacial–Holocene sea surface temperatures and gradients between the North Atlantic and the Norwegian Sea: Implications for the Nordic heat pump, *Geol. Soc. Spec. Publ.*, *111*, 177–185.

Labeyrie, L. (1990), PALEOCINAT (Paleocirculation de l'Atlantique nord), preliminary report, Inst. Fr. de Rech. Pout l'Exploit. de la Mer, Brest, France.

Labeyrie, L., et al. (1995), Surface and deep hydrology of the northern Atlantic Ocean during the past 150 000 years, *Philos. Trans. R. Soc. London, Ser. B*, *348*, 255–264.

Labeyrie, L., H. Leclaire, C. Waelbroeck, E. Cortijo, J.-C. Duplessy, L. Vidal, M. Elliot, and B. Le Coat (1999), Temporal variability of the surface and deep waters of the north west Atlantic Ocean at orbital and millennial scales, in *Mechanisms of Global Climate Change at Millennial Time Scales*, *Geophys. Monogr. Ser.*, vol. 122, edited by P. U. Clark, R. S. Webb, and L. D. Keigwin, pp. 77–98, AGU, Washington, D. C.

Laj, C., C. Kissel, A. Mazaud, J. E. T. Channell, and J. Beer (2000), North Atlantic palaeointensity stack since 75 ka (NAPIS-75) and the duration of the Laschamp event, *Philos. Trans. R. Soc. London, Ser. A*, *358*, 1009–1025.

Longhurst, A. (1998), *Ecological Geography of the Sea*, 398 pp., Elsevier, New York.

Manighetti, B. (1993), The glacial to Holocene sedimentary regime in the northeast Atlantic Ocean, Ph.D. thesis, Univ. of Cambridge, Cambridge, U. K.

Manthé, S., (1998), Variabilité de la circulation thermohaline glaciaire et interglaciaire tracée par les foraminifères planctoniques et de la microfaune benthique, Ph.D. thesis, Univ. Bordeaux I, Bordeaux, France.

Marchitto, T. M., Jr., D. W. Oppo, and W. B. Curry (2002), Paired benthic foraminiferal Cd/Ca and Zn/Ca evidence for a greatly increased presence of Southern Ocean water in the glacial North Atlantic, *Paleoceanography*, *17*(3), 1038, doi:10.1029/2000PA000598.

Marshall, J., Y. Kushnir, D. Battisti, P. Chang, A. Czaja, R. Dickson, J. Hurrell, M. McCartney, R. Saravanan, and M. Visbeck (2001), North Atlantic climate variability: Phenomena, impacts and mechanisms, *Int. J. Climatol.*, *21*, 1863–1898.

Maslin, M. A., N. J. Shackleton, and U. Pflaumann (1995), Surface water temperature, salinity, and density changes in the northeast Atlantic during the last 45,000 years: Heinrich events, deep water formation, and climatic rebounds, *Paleoceanography*, *10*, 527–544.

McCartney, M. S., S. L. Bennett, and M. E. Woodgate-Jones (1991), Eastward flow through the Mid-Atlantic Ridge at 11°N and its influence on the abyss of the Eastern basin, *J. Phys. Oceanogr.*, *21*, 1089–1121.

McManus, J. F., R. Francois, J.-M. Gherardi, L. D. Keigwin, and S. Brown-Leger (2004), Collapse and rapid resumption of Atlantic meridional circulation linked to deglacial climate changes, *Nature*, *428*, 834–837.

Oppo, D. W., and S. J. Lehman (1995), Suborbital timescale variability of North Atlantic Deep Water during the past 200,000 years, *Paleoceanography*, *10*, 901–910.

Ostermann, D. R., and W. B. Curry (2000), Calibration of stable isotopic data: An enriched $\delta^{18}O$ standard used for source gas mixing detection and correction, *Paleoceanography*, *15*, 353–360.

Paillard, D., L. Labeyrie, and P. Yiou (1996), Macintosh program performs time-series analysis, *Eos Trans. AGU*, *77*, 379.

Parsons, T. R., and C. M. Lalli (1988), Comparative oceanic ecology of the plankton communities of the subarctic Atlantic and Pacific oceans, *Oceanogr. Mar. Biol.*, *26*, 317–359.

Pastouret, L., G. A. Auffret, M. Hoffert, M. Melguen, H. D. Needham, and C. Latouche (1975), Sédimentation sur la Ride de Terre-Neuve, *Can. J. Earth Sci.*, *12*, 1019–1035.

Rasmussen, T. L., E. Thomsen, T. C. E. van Weering, and L. Labeyrie (1996), Rapid changes in surface and deep water conditions at the Faeroe Margin during the last 58,000 years, *Paleoceanography*, *11*, 757–771.

Reynolds-Sautter, L., and R. C. Thunell (1989), Seasonal succession of planktonic foraminifera: Results from a four-year time-series sediment trap experiment in the northeast Pacific, *J. Foraminiferal Res.*, *19*, 253–267.

Ruddiman, W. F. (1977), Late Quaternary deposition of ice-rafted sand in the subpolar North Atlantic (lat 40° to 65°N), *Geol. Soc. Am. Bull.*, *88*, 1813–1827.

Ruddiman, W. F., and A. McIntyre (1981), The North Atlantic Ocean during the last deglaciation, *Palaeoceanogr. Palaeoclimatol. Palaeoecol.*, *35*, 145–214.

Rühlemann, C., P. J. Müller, and R. R. Schneider (1999), Organic carbon and carbonate as paleoproductivity proxies: Examples from high and low productivity areas of the tropical Atlantic, in *Use of Proxies in Paleoceanography: Examples From the South Atlantic*, edited by G. Fischer and G. Wefer, pp. 315–344, Springer, New York.

Sancetta, C. (1992), Primary production in the glacial North Atlantic and North Pacific oceans, *Nature*, *360*, 249–251.

Schrader, H.-J., and G. Schuette (1968), Marine diatoms, in *The Sea*, edited by C. Emiliani, pp. 1179–1231, John Wiley, Hoboken, N. J.

Shackleton, N. J. (1974), Attainment of isotopic equilibrium between ocean water and the benthonic foraminifera genus Uvigerina: Isotopic changes in the ocean during the last glacial, in *Les méthodes quantitatives d'étude des variations du climat au cours du pléistocène*, pp. 203–210, Gif/Yvette Colloq. Int. du Cent. Natl. de la Rech. Sci., Paris.

Stuiver, M., and T. F. Braziunas (1993), Sun, ocean, climate and atmosphere $^{14}CO_2$: An evaluation of causal and spectral relationships, *Holocene*, *3*, 289–305.

Stuiver, M., P. J. Reimer, E. Bard, J. W. Beck, G. S. Burr, K. A. Hughen, B. Kromer, F. G. McCormac, J. Plicht, and M. Spurk (1998a), INTCAL98 radiocarbon age calibration 24,000-0 cal BP, *Radiocarbon*, *40*, 1041–1083.

Stuiver, M., P. J. Reimer, and T. F. Braziunas (1998b), High-precision radiocarbon age calibration for terrestrial and marine samples, *Radiocarbon*, *40*, 1127–1151.

Sverdrup, H. U. (1953), On conditions of the vernal blooming of phytoplankton, *J. Cons. Cons. Int. Explor. Mer*, *18*, 287–295.

Thomas, E., L. Booth, M. Maslin, and N. J. Shackleton (1995), Northeastern Atlantic benthic foraminifera during the last 45,000 years: Changes in productivity seen from the bottom up, *Paleoceanography*, *10*, 545–562.

Vautravers, M. (1997), Sédimentation et dissolution des carbonates biogéniques aux moyennes latitudes Nord et Sud: Approche quantitative et relations avec les paléocirculations océaniques des derniers 150,000 ans, Ph.D. thesis, Univ. Bordeaux I, Bordeaux, France.

Vidal, L., L. Labeyrie, E. Cortijo, M. Arnold, J. C. Duplessy, E. Michel, S. Becqué, and T. C. E. van Weering (1997), Evidence for changes in the North Atlantic Deep Water linked to meltwater surges during the Heinrich events, *Earth Planet. Sci. Lett.*, *146*, 13–27.

Villanueva, J., J. O. Grimalt, E. Cortijo, L. Vidal, and L. Labeyrie (1997), A biomarker approach to the organic matter deposited in the North Atlantic during the last climatic cycle, *Geochim. Cosmochim. Acta*, *61*, 4633–4646.

Waelbroeck, C., J.-C. Duplessy, E. Michel, L. Labeyrie, D. Paillard, and J. Duprat (2001), The timing of the last deglaciation in North Atlantic climate records, *Nature*, *412*, 724–727.

Wagner, T., and L. M. Dupont (1999), Terrestrial organic matter in marine sediments: Analytical approaches and eolian-marine records in the central equatorial Atlantic, in *Use of Proxies in Paleoceanography: Examples From the South Atlantic*, edited by G. Fischer and G. Wefer, pp. 547–574, Springer, New York.

Weeks, R. J., C. Laj, L. Endignoux, A. Mazaud, L. Labeyrie, A. P. Roberts, C. Kissel, and E. Blanchard (1995), Normalized natural remanent magnetisation intensity during the last 240,000 years in piston cores from the central North Atlantic Ocean: Geomagnetic field intensity or environmental signal?, *Phys. Earth Planet. Inter.*, *87*, 213–229.

Wefer, G., W. H. Berger, J. Bijma, and G. Fischer (1999), Clues to ocean history: A brief overview of proxies, in *Use of Proxies in Paleoceanography: Examples From the South Atlantic*, edited by G. Fischer and G. Wefer, pp. 1–68, Springer, New York.

Yu, E.-F., R. Francois, M. P. Bacon, and A. P. Fleer (2001), Fluxes of ^{230}Th and ^{231}Pa to the deep sea: Implications for the interpretation of excess ^{230}Th and $^{231}Pa/^{230}Th$ profiles in sediments, *Earth Planet. Sci. Lett.*, *191*, 219–230.

F. Abrantes and S. Nave, Departamento de Geologia Marinha, Instituto Nacional de Engenharia, Tecnologia e Inovação, Alfragide, Portugal. (silvia.nave@ineti.pt)

N. Caillon, E. Cortijo, J. Gherardi, C. Kissel, and L. Labeyrie, Laboratoire des Sciences du Climat et de l'Environnement, CEA/CNRS/UVSQ, Gif-sur-Yvette, France.